
QSGD: Communication-Efficient SGD via Gradient Quantization and Encoding

Dan Alistarh
IST Austria & ETH Zurich
dan.alistarh@ist.ac.at

Demjan Grubic
ETH Zurich & Google
demjangrubic@gmail.com

Jerry Z. Li
MIT
jerryzli@mit.edu

Ryota Tomioka
Microsoft Research
ryoto@microsoft.com

Milan Vojnovic
London School of Economics
M.Vojnovic@lse.ac.uk

Abstract

Parallel implementations of stochastic gradient descent (SGD) have received significant research attention, thanks to its excellent scalability properties. A fundamental barrier when parallelizing SGD is the high bandwidth cost of communicating gradient updates between nodes; consequently, several lossy compression heuristics have been proposed, by which nodes only communicate *quantized* gradients. Although effective in practice, these heuristics do not always converge.

In this paper, we propose *Quantized SGD (QSGD)*, a family of compression schemes with convergence guarantees and good practical performance. QSGD allows the user to smoothly trade off *communication bandwidth* and *convergence time*: nodes can adjust the number of bits sent per iteration, at the cost of possibly higher variance. We show that this trade-off is inherent, in the sense that improving it past some threshold would violate information-theoretic lower bounds. QSGD guarantees convergence for convex and non-convex objectives, under asynchrony, and can be extended to stochastic variance-reduced techniques.

When applied to training deep neural networks for image classification and automated speech recognition, QSGD leads to significant reductions in end-to-end training time. For instance, on 16GPUs, we can train the ResNet-152 network to full accuracy on ImageNet 1.8× faster than the full-precision variant.

1 Introduction

The surge of massive data has led to significant interest in *distributed* algorithms for scaling computations in the context of machine learning and optimization. In this context, much attention has been devoted to scaling large-scale *stochastic gradient descent* (SGD) algorithms [33], which can be briefly defined as follows. Let $f : \mathbb{R}^n \rightarrow \mathbb{R}$ be a function which we want to minimize. We have access to stochastic gradients \tilde{g} such that $\mathbb{E}[\tilde{g}(\mathbf{x})] = \nabla f(\mathbf{x})$. A standard instance of SGD will converge towards the minimum by iterating the procedure

$$\mathbf{x}_{t+1} = \mathbf{x}_t - \eta_t \tilde{g}(\mathbf{x}_t), \quad (1)$$

where \mathbf{x}_t is the current candidate, and η_t is a variable step-size parameter. Notably, this arises if we are given i.i.d. data points X_1, \dots, X_m generated from an unknown distribution D , and a loss function $\ell(X, \theta)$, which measures the loss of the model θ at data point X . We wish to find a model θ^* which minimizes $f(\theta) = \mathbb{E}_{X \sim D}[\ell(X, \theta)]$, the expected loss to the data. This framework captures many fundamental tasks, such as neural network training.

In this paper, we focus on *parallel* SGD methods, which have received considerable attention recently due to their high scalability [6, 8, 13, 32]. Specifically, we consider a setting where a large dataset is partitioned among K processors, which collectively minimize a function f . Each processor maintains a local copy of the parameter vector \mathbf{x}_t ; in each iteration, it obtains a new stochastic gradient update (corresponding to its local data). Processors then broadcast their gradient updates to their peers, and aggregate the gradients to compute the new iterate \mathbf{x}_{t+1} .

In most current implementations of parallel SGD, in each iteration, each processor must communicate its entire gradient update to all other processors. If the gradient vector is dense, each processor will need to send and receive n floating-point numbers *per iteration* to/from each peer to communicate the gradients and maintain the parameter vector \mathbf{x} . In practical applications, communicating the gradients in each iteration has been observed to be a significant performance bottleneck [8, 35, 37].

One popular way to reduce this cost has been to perform *lossy compression of the gradients* [1, 3, 10, 11, 41]. A simple implementation is to simply *reduce precision* of the representation, which has been shown to converge under convexity and sparsity assumptions [10]. A more drastic quantization technique is *1BitSGD* [35, 37], which reduces each component of the gradient to *just its sign* (one bit), scaled by the average over the coordinates of $\tilde{\mathbf{g}}$, accumulating errors locally. 1BitSGD was experimentally observed to preserve convergence [35], under certain conditions; thanks to the reduction in communication, it enabled state-of-the-art scaling of deep neural networks (DNNs) for acoustic modelling [37]. However, it is currently not known if 1BitSGD provides any guarantees, even under strong assumptions, and it is not clear if higher compression is achievable.

Contributions. Our focus is understanding the trade-offs between the *communication cost* of data-parallel SGD, and its *convergence guarantees*. We propose a family of algorithms allowing for lossy compression of gradients called *Quantized SGD (QSGD)*, by which processors can trade-off the number of bits communicated per iteration with the variance added to the process.

QSGD is built on two algorithmic ideas. The first is an intuitive *stochastic quantization* scheme: given the gradient vector at a processor, we *quantize* each component by randomized rounding to a discrete set of values, in a principled way which preserves the statistical properties of the original. The second step is an efficient lossless code for quantized gradients, which exploits their statistical properties to generate efficient encodings. Our analysis gives tight bounds on the precision-variance trade-off induced by QSGD.

At one extreme of this trade-off, we can guarantee that each processor transmits at most $\sqrt{n}(\log n + O(1))$ expected bits per iteration, while increasing variance by at most a \sqrt{n} multiplicative factor. At the other extreme, we show that each processor can transmit $\leq 2.8n + 32$ bits per iteration in expectation, while increasing variance by a only a factor of 2. In particular, in the latter regime, compared to full precision SGD, we use $\approx 2.8n$ bits of communication per iteration as opposed to $32n$ bits, and guarantee at most $2\times$ more iterations, leading to bandwidth savings of $\approx 5.7\times$.

QSGD is fairly general: it can also be shown to converge, under assumptions, to local minima for non-convex objectives, as well as under asynchronous iterations. One non-trivial extension we develop is a *stochastic variance-reduced* [23] variant of QSGD, called QSVRG, which has exponential convergence rate.

One key question is whether QSGD’s compression-variance trade-off is *inherent*: for instance, does any algorithm guaranteeing at most constant variance blowup need to transmit $\Omega(n)$ bits per iteration? The answer is positive: improving asymptotically upon this trade-off would break the communication complexity lower bound of distributed mean estimation (see [44, Proposition 2] and [38]).

Experiments. The crucial question is whether, in practice, QSGD can reduce communication cost by enough to offset the overhead of any additional iterations to convergence. The answer is yes. We explore the practicality of QSGD on a variety of state-of-the-art datasets and machine learning models: we examine its performance in training networks for image classification tasks (AlexNet, Inception, ResNet, and VGG) on the ImageNet [12] and CIFAR-10 [25] datasets, as well as on LSTMs [19] for speech recognition. We implement QSGD in Microsoft CNTK [3].

Experiments show that all these models can significantly benefit from reduced communication when doing multi-GPU training, *with virtually no accuracy loss*, and *under standard parameters*. For example, when training AlexNet on 16 GPUs with standard parameters, the reduction in communication time is $4\times$, and the reduction in training to the network’s top accuracy is $2.5\times$. When training an LSTM on two GPUs, the reduction in communication time is $6.8\times$, while the reduction in training

time to the same target accuracy is $2.7\times$. Further, even computationally-heavy architectures such as Inception and ResNet can benefit from the reduction in communication: on 16GPUs, QSGD reduces the end-to-end convergence time of ResNet152 by approximately $2\times$. Networks trained with QSGD can converge to virtually the same accuracy as full-precision variants, and that gradient quantization may even slightly *improve* accuracy in some settings.

Related Work. One line of related research studies the *communication complexity* of convex optimization. In particular, [40] studied two-processor convex minimization in the same model, provided a lower bound of $\Omega(n(\log n + \log(1/\epsilon)))$ bits on the communication cost of n -dimensional convex problems, and proposed a *non-stochastic* algorithm for strongly convex problems, whose communication cost is within a log factor of the lower bound. By contrast, our focus is on *stochastic* gradient methods. Recent work [5] focused on *round complexity* lower bounds on the number of *communication rounds* necessary for convex learning.

Buckwild! [10] was the first to consider the convergence guarantees of low-precision SGD. It gave upper bounds on the error probability of SGD, assuming unbiased stochastic quantization, convexity, and gradient sparsity, and showed significant speedup when solving convex problems on CPUs. QSGD refines these results by focusing on the trade-off between communication and convergence. We view quantization as an independent source of variance for SGD, which allows us to employ standard convergence results [7]. The main differences from Buckwild! are that 1) we focus on the variance-precision trade-off; 2) our results apply to the quantized non-convex case; 3) we validate the practicality of our scheme on neural network training on GPUs. Concurrent work proposes TernGrad [41], which starts from a similar stochastic quantization, but focuses on the case where individual gradient components can have only three possible values. They show that significant speedups can be achieved on TensorFlow [1], while maintaining accuracy within a few percentage points relative to full precision. The main differences to our work are: 1) our implementation guarantees convergence under standard assumptions; 2) we strive to provide a black-box compression technique, with no additional hyperparameters to tune; 3) experimentally, QSGD maintains the same accuracy within the same target number of epochs; for this, we allow gradients to have larger bit width; 4) our experiments focus on the single-machine multi-GPU case.

We note that QSGD can be applied to solve the distributed mean estimation problem [24, 38] with an optimal error-communication trade-off in some regimes. In contrast to the elegant random rotation solution presented in [38], QSGD employs quantization and Elias coding. Our use case is different from the federated learning application of [24, 38], and has the advantage of being more efficient to compute on a GPU.

There is an extremely rich area studying algorithms and systems for efficient distributed large-scale learning, e.g. [1, 3, 6, 10, 11, 21, 32, 39, 43]. Significant interest has recently been dedicated to *quantized* frameworks, both for inference, e.g., [1, 17] and training [10, 16, 20, 35, 37, 42, 45]. In this context, [35] proposed 1BitSGD, a heuristic for compressing gradients in SGD, inspired by delta-sigma modulation [34]. It is implemented in Microsoft CNTK, and has a cost of n bits and two floats per iteration. Variants of it were shown to perform well on large-scale Amazon datasets by [37]. Compared to 1BitSGD, QSGD can achieve asymptotically higher compression, provably converges under standard assumptions, and shows superior practical performance in some cases.

2 Preliminaries

SGD has many variants, with different preconditions and guarantees. Our techniques are rather portable, and can usually be applied in a black-box fashion on top of SGD. For conciseness, we will focus on a basic SGD setup. The following assumptions are standard; see e.g. [7].

Let $\mathcal{X} \subseteq \mathbb{R}^n$ be a known convex set, and let $f : \mathcal{X} \rightarrow \mathbb{R}$ be differentiable, convex, smooth, and unknown. We assume repeated access to stochastic gradients of f , which on (possibly random) input \mathbf{x} , outputs a direction which is in expectation the correct direction to move in. Formally:

Definition 2.1. Fix $f : \mathcal{X} \rightarrow \mathbb{R}$. A *stochastic gradient* for f is a random function $\tilde{g}(\mathbf{x})$ so that $\mathbb{E}[\tilde{g}(\mathbf{x})] = \nabla f(\mathbf{x})$. We say the stochastic gradient has second moment at most B if $\mathbb{E}[\|\tilde{g}\|_2^2] \leq B$ for all $x \in \mathcal{X}$. We say it has variance at most σ^2 if $\mathbb{E}[\|\tilde{g}(\mathbf{x}) - \nabla f(\mathbf{x})\|_2^2] \leq \sigma^2$ for all $x \in \mathcal{X}$.

Observe that any stochastic gradient with second moment bound B is automatically also a stochastic gradient with variance bound $\sigma^2 = B$, since $\mathbb{E}[\|\tilde{g}(\mathbf{x}) - \nabla f(\mathbf{x})\|_2^2] \leq \mathbb{E}[\|\tilde{g}(\mathbf{x})\|_2^2]$ as long as $\mathbb{E}[\tilde{g}(\mathbf{x})] = \nabla f(\mathbf{x})$. Second, in convex optimization, one often assumes a second moment bound

Data: Local copy of the parameter vector \mathbf{x}

```

1 for each iteration  $t$  do
2   Let  $\tilde{g}_t^i$  be an independent stochastic gradient ;
3    $M^i \leftarrow \text{Encode}(\tilde{g}_t^i(\mathbf{x}))$  //encode gradients ;
4   broadcast  $M^i$  to all peers;
5   for each peer  $\ell$  do
6     receive  $M^\ell$  from peer  $\ell$ ;
7      $\hat{g}^\ell \leftarrow \text{Decode}(M^\ell)$  //decode gradients ;
8   end
9    $\mathbf{x}_{t+1} \leftarrow \mathbf{x}_t - (\eta_t/K) \sum_{\ell=1}^K \hat{g}^\ell$ ;
10 end

```

Algorithm 1: Parallel SGD Algorithm.

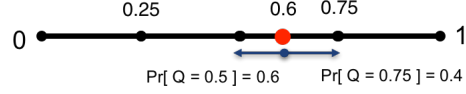


Figure 1: An illustration of generalized stochastic quantization with 5 levels.

when dealing with non-smooth convex optimization, and a variance bound when dealing with smooth convex optimization. However, for us it will be convenient to consistently assume a second moment bound. This does not seem to be a major distinction in theory or in practice [7].

Given access to stochastic gradients, and a starting point \mathbf{x}_0 , SGD builds iterates \mathbf{x}_t given by Equation (1), projected onto \mathcal{X} , where $(\eta_t)_{t \geq 0}$ is a sequence of step sizes. In this setting, one can show:

Theorem 2.1 ([7], Theorem 6.3). *Let $\mathcal{X} \subseteq \mathbb{R}^n$ be convex, and let $f : \mathcal{X} \rightarrow \mathbb{R}$ be unknown, convex, and L -smooth. Let $\mathbf{x}_0 \in \mathcal{X}$ be given, and let $R^2 = \sup_{\mathbf{x} \in \mathcal{X}} \|\mathbf{x} - \mathbf{x}_0\|^2$. Let $T > 0$ be fixed. Given repeated, independent access to stochastic gradients with variance bound σ^2 for f , SGD with initial point \mathbf{x}_0 and constant step sizes $\eta_t = \frac{1}{L+1/\gamma}$, where $\gamma = \frac{R}{\sigma} \sqrt{\frac{2}{T}}$, achieves*

$$\mathbb{E} \left[f \left(\frac{1}{T} \sum_{t=0}^T \mathbf{x}_t \right) \right] - \min_{\mathbf{x} \in \mathcal{X}} f(\mathbf{x}) \leq R \sqrt{\frac{2\sigma^2}{T}} + \frac{LR^2}{T}. \quad (2)$$

Minibatched SGD. A modification to the SGD scheme presented above often observed in practice is a technique known as *minibatching*. In minibatched SGD, updates are of the form $\mathbf{x}_{t+1} = \Pi_{\mathcal{X}}(\mathbf{x}_t - \eta_t \tilde{G}_t(\mathbf{x}_t))$, where $\tilde{G}_t(\mathbf{x}_t) = \frac{1}{m} \sum_{i=1}^m \tilde{g}_{t,i}$, and where each $\tilde{g}_{t,i}$ is an independent stochastic gradient for f at \mathbf{x}_t . It is not hard to see that if $\tilde{g}_{t,i}$ are stochastic gradients with variance bound σ^2 , then the \tilde{G}_t is a stochastic gradient with variance bound σ^2/m . By inspection of Theorem 2.1, as long as the first term in (2) dominates, minibatched SGD requires $1/m$ fewer iterations to converge.

Data-Parallel SGD. We consider synchronous *data-parallel* SGD, modelling real-world multi-GPU systems, and focus on the communication cost of SGD in this setting. We have a set of K processors p_1, p_2, \dots, p_K who proceed in synchronous steps, and communicate using point-to-point messages. Each processor maintains a local copy of a vector \mathbf{x} of dimension n , representing the current estimate of the minimizer, and has access to private, independent stochastic gradients for f .

In each synchronous iteration, described in Algorithm 1, each processor aggregates the value of \mathbf{x} , then obtains random gradient updates for each component of \mathbf{x} , then communicates these updates to all peers, and finally aggregates the received updates and applies them locally. Importantly, we add *encoding* and *decoding* steps for the gradients before and after send/receive in lines 3 and 7, respectively. In the following, whenever describing a variant of SGD, we assume the above general pattern, and only specify the *encode/decode* functions. Notice that the decoding step does not necessarily recover the original gradient \tilde{g}^ℓ ; instead, we usually apply an *approximate* version.

When the encoding and decoding steps are the identity (i.e., no encoding / decoding), we shall refer to this algorithm as *parallel SGD*. In this case, it is a simple calculation to see that at each processor, if \mathbf{x}_t was the value of \mathbf{x} that the processors held before iteration t , then the updated value of \mathbf{x} by the end of this iteration is $\mathbf{x}_{t+1} = \mathbf{x}_t - (\eta_t/K) \sum_{\ell=1}^K \tilde{g}^\ell(\mathbf{x}_t)$, where each \tilde{g}^ℓ is a stochastic gradient. In particular, this update is merely a minibatched update of size K . Thus, by the discussion above, and by rephrasing Theorem 2.1, we have the following corollary:

Corollary 2.2. *Let $\mathcal{X}, f, L, \mathbf{x}_0$, and R be as in Theorem 2.1. Fix $\epsilon > 0$. Suppose we run parallel SGD on K processors, each with access to independent stochastic gradients with second moment*

bound B , with step size $\eta_t = 1/(L + \sqrt{K}/\gamma)$, where γ is as in Theorem 2.1. Then if

$$T = O\left(R^2 \cdot \max\left(\frac{2B}{K\epsilon^2}, \frac{L}{\epsilon}\right)\right), \text{ then } \mathbb{E}\left[f\left(\frac{1}{T}\sum_{t=0}^T \mathbf{x}_t\right)\right] - \min_{\mathbf{x} \in \mathcal{X}} f(\mathbf{x}) \leq \epsilon. \quad (3)$$

In most reasonable regimes, the first term of the max in (3) will dominate the number of iterations necessary. Specifically, the number of iterations will depend linearly on the second moment bound B .

3 Quantized Stochastic Gradient Descent (QSGD)

In this section, we present our main results on stochastically quantized SGD. Throughout, \log denotes the base-2 logarithm, and the number of bits to represent a float is 32. For any vector $\mathbf{v} \in \mathbb{R}^n$, we let $\|\mathbf{v}\|_0$ denote the number of nonzeros of \mathbf{v} . For any string $\omega \in \{0, 1\}^*$, we will let $|\omega|$ denote its length. For any scalar $x \in \mathbb{R}$, we let $\text{sgn}(x) \in \{-1, +1\}$ denote its sign, with $\text{sgn}(0) = 1$.

3.1 Generalized Stochastic Quantization and Coding

Stochastic Quantization. We now consider a general, parametrizable lossy-compression scheme for stochastic gradient vectors. The quantization function is denoted with $Q_s(\mathbf{v})$, where $s \geq 1$ is a tuning parameter, corresponding to the number of quantization levels we implement. Intuitively, we define s uniformly distributed levels between 0 and 1, to which each value is quantized in a way which preserves the value in expectation, and introduces minimal variance. Please see Figure 1.

For any $\mathbf{v} \in \mathbb{R}^n$ with $\mathbf{v} \neq \mathbf{0}$, $Q_s(\mathbf{v})$ is defined as

$$Q_s(v_i) = \|\mathbf{v}\|_2 \cdot \text{sgn}(v_i) \cdot \xi_i(\mathbf{v}, s), \quad (4)$$

where $\xi_i(\mathbf{v}, s)$'s are independent random variables defined as follows. Let $0 \leq \ell < s$ be an integer such that $|v_i|/\|\mathbf{v}\|_2 \in [\ell/s, (\ell+1)/s]$. That is, $[\ell/s, (\ell+1)/s]$ is the quantization interval corresponding to $|v_i|/\|\mathbf{v}\|_2$. Then

$$\xi_i(\mathbf{v}, s) = \begin{cases} \ell/s & \text{with probability } 1 - p\left(\frac{|v_i|}{\|\mathbf{v}\|_2}, s\right); \\ (\ell+1)/s & \text{otherwise.} \end{cases}$$

Here, $p(a, s) = as - \ell$ for any $a \in [0, 1]$. If $\mathbf{v} = \mathbf{0}$, then we define $Q(\mathbf{v}, s) = \mathbf{0}$.

The distribution of $\xi_i(\mathbf{v}, s)$ has minimal variance over distributions with support $\{0, 1/s, \dots, 1\}$, and its expectation satisfies $\mathbb{E}[\xi_i(\mathbf{v}, s)] = |v_i|/\|\mathbf{v}\|_2$. Formally, we can show:

Lemma 3.1. *For any vector $\mathbf{v} \in \mathbb{R}^n$, we have that (i) $\mathbb{E}[Q_s(\mathbf{v})] = \mathbf{v}$ (unbiasedness), (ii) $\mathbb{E}[\|Q_s(\mathbf{v}) - \mathbf{v}\|_2^2] \leq \min(n/s^2, \sqrt{n}/s)\|\mathbf{v}\|_2^2$ (variance bound), and (iii) $\mathbb{E}[\|Q_s(\mathbf{v})\|_0] \leq s(s + \sqrt{n})$ (sparsity).*

Efficient Coding of Gradients. Observe that for any vector \mathbf{v} , the output of $Q_s(\mathbf{v})$ is naturally expressible by a tuple $(\|\mathbf{v}\|_2, \boldsymbol{\sigma}, \boldsymbol{\zeta})$, where $\boldsymbol{\sigma}$ is the vector of signs of the v_i 's and $\boldsymbol{\zeta}$ is the vector of integer values $s \cdot \xi_i(\mathbf{v}, s)$. The key idea behind the coding scheme is that not all integer values $s \cdot \xi_i(\mathbf{v}, s)$ can be equally likely: in particular, *larger integers are less frequent*. We will exploit this via a specialized *Elias* integer encoding [14].

Intuitively, for any positive integer k , its code, denoted $\text{Elias}(k)$, starts from the binary representation of k , to which it prepends the *length* of this representation. It then recursively encodes this prefix. We show that for any positive integer k , the length of the resulting code has $|\text{Elias}(k)| = \log k + \log \log k + \dots + 1 \leq (1 + o(1)) \log k + 1$, and that encoding and decoding can be done efficiently.

Given a gradient vector represented as the triple $(\|\mathbf{v}\|_2, \boldsymbol{\sigma}, \boldsymbol{\zeta})$, with s quantization levels, our coding outputs a string S defined as follows. First, it uses 32 bits to encode $\|\mathbf{v}\|_2$. It proceeds to encode using Elias recursive coding the position of the first nonzero entry of $\boldsymbol{\zeta}$. It then appends a bit denoting σ_i and follows that with $\text{Elias}(s \cdot \xi_i(\mathbf{v}, s))$. Iteratively, it proceeds to encode the distance from the current coordinate of $\boldsymbol{\zeta}$ to the next nonzero, and encodes the σ_i and ζ_i for that coordinate in the same way. The decoding scheme is straightforward: we first read off 32 bits to construct $\|\mathbf{v}\|_2$, then iteratively use the decoding scheme for Elias recursive coding to read off the positions and values of the nonzeros of $\boldsymbol{\zeta}$ and $\boldsymbol{\sigma}$. The properties of the quantization and of the encoding imply the following.

Theorem 3.2. *Let $f : \mathbb{R}^n \rightarrow \mathbb{R}$ be fixed, and let $\mathbf{x} \in \mathbb{R}^n$ be arbitrary. Fix $s \geq 2$ quantization levels. If $\tilde{g}(\mathbf{x})$ is a stochastic gradient for f at \mathbf{x} with second moment bound B , then $Q_s(\tilde{g}(\mathbf{x}))$ is a*

stochastic gradient for f at \mathbf{x} with variance bound $\min\left(\frac{n}{s^2}, \frac{\sqrt{n}}{s}\right) B$. Moreover, there is an encoding scheme so that in expectation, the number of bits to communicate $Q_s(\tilde{g}(\mathbf{x}))$ is upper bounded by

$$\left(3 + \left(\frac{3}{2} + o(1)\right) \log\left(\frac{2(s^2 + n)}{s(s + \sqrt{n})}\right)\right) s(s + \sqrt{n}) + 32.$$

Sparse Regime. For the case $s = 1$, i.e., quantization levels 0, 1, and -1 , the gradient density is $O(\sqrt{n})$, while the second-moment blowup is $\leq \sqrt{n}$. Intuitively, this means that we will employ $O(\sqrt{n} \log n)$ bits per iteration, while the convergence time is increased by $O(\sqrt{n})$.

Dense Regime. The variance blowup is minimized to at most **2** for $s = \sqrt{n}$ quantization levels; in this case, we devise a more efficient encoding which yields an order of magnitude shorter codes compared to the full-precision variant. The proof of this statement is not entirely obvious, as it exploits both the statistical properties of the quantization and the guarantees of the Elias coding.

Corollary 3.3. *Let f , \mathbf{x} , and $\tilde{g}(\mathbf{x})$ be as in Theorem 3.2. There is an encoding scheme for $Q_{\sqrt{n}}(\tilde{g}(\mathbf{x}))$ which in expectation has length at most $2.8n + 32$.*

3.2 QSGD Guarantees

Putting the bounds on the communication and variance given above with the guarantees for SGD algorithms on smooth, convex functions yield the following results:

Theorem 3.4 (Smooth Convex QSGD). *Let \mathcal{X} , f , L , \mathbf{x}_0 , and R be as in Theorem 2.1. Fix $\epsilon > 0$. Suppose we run parallel QSGD with s quantization levels on K processors accessing independent stochastic gradients with second moment bound B , with step size $\eta_t = 1/(L + \sqrt{K}/\gamma)$, where γ is as in Theorem 2.1 with $\sigma = B'$, where $B' = \min\left(\frac{n}{s^2}, \frac{\sqrt{n}}{s}\right) B$. Then if $T = O\left(R^2 \cdot \max\left(\frac{2B'}{K\epsilon^2}, \frac{L}{\epsilon}\right)\right)$, then $\mathbb{E}\left[f\left(\frac{1}{T} \sum_{t=0}^T \mathbf{x}_t\right)\right] - \min_{\mathbf{x} \in \mathcal{X}} f(\mathbf{x}) \leq \epsilon$. Moreover, QSGD requires $\left(3 + \left(\frac{3}{2} + o(1)\right) \log\left(\frac{2(s^2 + n)}{s^2 + \sqrt{n}}\right)\right) (s^2 + \sqrt{n}) + 32$ bits of communication per round. In the special case when $s = \sqrt{n}$, this can be reduced to $2.8n + 32$.*

QSGD is quite portable, and can be applied to almost any stochastic gradient method. For illustration, we can use quantization along with [15] to get communication-efficient non-convex SGD.

Theorem 3.5 (QSGD for smooth non-convex optimization). *Let $f : \mathbb{R}^n \rightarrow \mathbb{R}$ be a L -smooth (possibly nonconvex) function, and let \mathbf{x}_1 be an arbitrary initial point. Let $T > 0$ be fixed, and $s > 0$. Then there is a random stopping time R supported on $\{1, \dots, N\}$ so that QSGD with quantization level s , constant stepsizes $\eta = O(1/L)$ and access to stochastic gradients of f with second moment bound B satisfies $\frac{1}{L} \mathbb{E}[\|\nabla f(\mathbf{x})\|_2^2] \leq O\left(\frac{\sqrt{L(f(\mathbf{x}_1) - f^*)}}{N} + \frac{\min(n/s^2, \sqrt{n}/s)B}{L}\right)$. Moreover, the communication cost is the same as in Theorem 3.4.*

3.3 Quantized Variance-Reduced SGD

Assume we are given K processors, and a parameter $m > 0$, where each processor i has access to functions $\{f_{im/K}, \dots, f_{(i+1)m/K-1}\}$. The goal is to approximately minimize $f = \frac{1}{m} \sum_{i=1}^m f_i$. For processor i , let $h_i = \frac{1}{m} \sum_{j=im/K}^{(i+1)m/K-1} f_j$ be the portion of f that it knows, so that $f = \sum_{i=1}^K h_i$.

A natural question is whether we can apply stochastic quantization to reduce communication for parallel SVRG. Upon inspection, we notice that the resulting update will break standard SVRG. We resolve this technical issue, proving one can quantize SVRG updates using our techniques and still obtain the same convergence bounds.

Algorithm Description. Let $\tilde{Q}(\mathbf{v}) = Q(\mathbf{v}, \sqrt{n})$, where $Q(\mathbf{v}, s)$ is defined as in Section 3.1. Given arbitrary starting point \mathbf{x}_0 , we let $\mathbf{y}^{(1)} = \mathbf{x}_0$. At the beginning of epoch p , each processor broadcasts $\nabla h_i(\mathbf{y}^{(p)})$, that is, the unquantized full gradient, from which the processors each aggregate $\nabla f(\mathbf{y}^{(p)}) = \sum_{i=1}^m \nabla h_i(\mathbf{y}^{(p)})$. Within each epoch, for each iteration $t = 1, \dots, T$, and for each processor $i = 1, \dots, K$, we let $j_{i,t}^{(p)}$ be a uniformly random integer from $[m]$ completely independent from everything else. Then, in iteration t in epoch p , processor i broadcasts the update vector $\mathbf{u}_{t,i}^{(p)} = \tilde{Q}\left(\nabla f_{j_{i,t}^{(p)}}(\mathbf{x}_t^{(p)}) - \nabla f_{j_{i,t}^{(p)}}(\mathbf{y}^{(p)}) + \nabla f(\mathbf{y}^{(p)})\right)$.

Table 1: Description of networks, final top-1 accuracy, as well as end-to-end training speedup on 8GPUs.

Network	Dataset	Params.	Init. Rate	Top-1 (32bit)	Top-1 (QSGD)	Speedup (8 GPUs)
AlexNet	ImageNet	62M	0.07	59.50%	60.05% (4bit)	2.05 ×
ResNet152	ImageNet	60M	1	77.0%	76.74% (8bit)	1.56 ×
ResNet50	ImageNet	25M	1	74.68%	74.76% (4bit)	1.26 ×
ResNet110	CIFAR-10	1M	0.1	93.86%	94.19% (4bit)	1.10 ×
BN-Inception	ImageNet	11M	3.6	-	-	1.16 × (projected)
VGG19	ImageNet	143M	0.1	-	-	2.25 × (projected)
LSTM	AN4	13M	0.5	81.13%	81.15 % (4bit)	2 × (2 GPUs)

Each processor then computes the total update $\mathbf{u}_t^{(p)} = \frac{1}{K} \sum_{i=1}^K \mathbf{u}_{t,i}$, and sets $\mathbf{x}_{t+1}^{(p)} = \mathbf{x}_t^{(p)} - \eta \mathbf{u}_t^{(p)}$. At the end of epoch p , each processor sets $\mathbf{y}^{(p+1)} = \frac{1}{T} \sum_{t=1}^T \mathbf{x}_t^{(p)}$. We can prove the following.

Theorem 3.6. *Let $f(\mathbf{x}) = \frac{1}{m} \sum_{i=1}^m f_i(\mathbf{x})$, where f is ℓ -strongly convex, and f_i are convex and L -smooth, for all i . Let \mathbf{x}^* be the unique minimizer of f over \mathbb{R}^n . Then, if $\eta = O(1/L)$ and $T = O(L/\ell)$, then QSVRG with initial point $\mathbf{y}^{(1)}$ ensures $\mathbb{E}[f(\mathbf{y}^{(p+1)})] - f(\mathbf{x}^*) \leq 0.9^p (f(\mathbf{y}^{(1)}) - f(\mathbf{x}^*))$, for any epoch $p \geq 1$. Moreover, QSVRG with T iterations per epoch requires $\leq (F + 2.8n)(T + 1) + Fn$ bits of communication per epoch.*

Discussion. In particular, this allows us to largely decouple the dependence between F and the condition number of f in the communication. Let $\kappa = L/\ell$ denote the condition number of f . Observe that whenever $F \ll \kappa$, the second term is subsumed by the first and the per epoch communication is dominated by $(F + 2.8n)(T + 1)$. Specifically, for any fixed ϵ , to attain accuracy ϵ we must take $F = O(\log 1/\epsilon)$. As long as $\log 1/\epsilon \geq \Omega(\kappa)$, which is true for instance in the case when $\kappa \geq \text{poly} \log(n)$ and $\epsilon \geq \text{poly}(1/n)$, then the communication per epoch is $O(\kappa(\log 1/\epsilon + n))$.

Gradient Descent. The full version of the paper [4] contains an application of QSGD to gradient descent. Roughly, in this case, QSGD can simply truncate the gradient to its top components, sorted by magnitude.

4 QSGD Variants

Our experiments will stretch the theory, as we use deep networks, with non-convex objectives. (We have also tested QSGD for convex objectives. Results closely follow the theory, and are therefore omitted.) Our implementations will depart from the previous algorithm description as follows.

First, we notice that we can control the variance the quantization by quantizing into *buckets* of a fixed size d . If we view each gradient as a one-dimensional vector \mathbf{v} , reshaping tensors if necessary, a *bucket* will be defined as a set of d consecutive vector values. (E.g. the i th bucket is the sub-vector $v[(i-1)d+1 : i \cdot d]$.) We will quantize each bucket *independently*, using QSGD. Setting $d = 1$ corresponds to no quantization (vanilla SGD), and $d = n$ corresponds to full quantization, as described in the previous section. It is easy to see that, using bucketing, the guarantees from Lemma 3.1 will be expressed in terms of d , as opposed to the full dimension n . This provides a knob by which we can control variance, at the cost of storing an extra scaling factor on every d bucket values. As an example, if we use a bucket size of 512, and 4 bits, the variance increase due to quantization will be upper bounded by only $\sqrt{512}/2^4 \simeq 1.41$. This provides a theoretical justification for the similar convergence rates we observe in practice.

The second difference from the theory is that we will scale by the *maximum* value of the vector (as opposed to the 2-norm). Intuitively, normalizing by the max preserves more values, and has slightly higher accuracy for the same number of iterations. Both methods have the same baseline bandwidth reduction because of lower bit width (e.g. 32 bits to 2 bits per dimension), but normalizing by the max no longer provides any sparsity guarantees. We note that this does not affect our bounds in the regime where we use $\Theta(\sqrt{n})$ quantization levels per component, as we employ no sparsity in that case. (However, we note that in practice max normalization also generates non-trivial sparsity.)

5 Experiments

Setup. We performed experiments on Amazon EC2 p2.16xlarge instances, with 16 NVIDIA K80 GPUs. Instances have GPUDirect peer-to-peer communication, but do not currently support NVIDIA

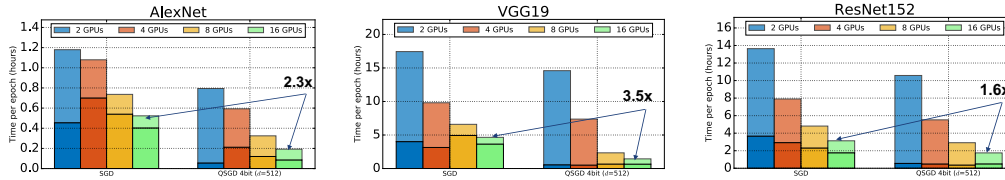


Figure 2: Breakdown of communication versus computation for various neural networks, on 2, 4, 8, 16 GPUs, for full 32-bit precision versus QSGD 4-bit. Each bar represents the total time for an epoch under standard parameters. Epoch time is broken down into *communication* (bottom, solid) and *computation* (top, transparent). Although epoch time *diminishes* as we parallelize, the proportion of communication *increases*.

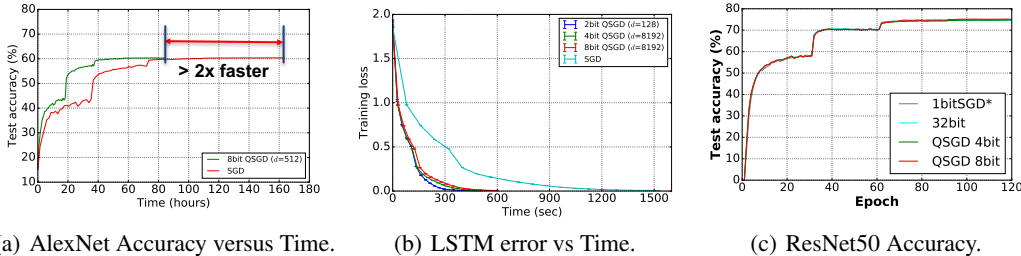


Figure 3: Accuracy numbers for different networks. Light blue lines represent 32-bit accuracy.

NCCL extensions. We have implemented QSGD on GPUs using the Microsoft Cognitive Toolkit (CNTK) [3]. This package provides efficient (MPI-based) GPU-to-GPU communication, and implements an optimized version of 1bit-SGD [35]. Our code is released as open-source [31].

We execute two types of tasks: *image classification* on ILSVRC 2015 (ImageNet) [12], CIFAR-10 [25], and MNIST [27], and *speech recognition* on the CMU AN4 dataset [2]. For vision, we experimented with AlexNet [26], VGG [36], ResNet [18], and Inception with Batch Normalization [22] deep networks. For speech, we trained an LSTM network [19]. See Table 1 for details.

Protocol. Our methodology emphasizes *zero error tolerance*, in the sense that we always aim to preserve the accuracy of the networks trained. We used standard sizes for the networks, with hyper-parameters optimized for the 32bit precision variant. (Unless otherwise stated, we use the default networks and hyper-parameters optimized for full-precision CNTK 2.0.) We increased batch size when necessary to balance communication and computation for larger GPU counts, but never past the point where we lose accuracy. We employed *double buffering* [35] to perform communication and quantization concurrently with the computation. Quantization usually benefits from lowering learning rates; yet, we always run the 32bit learning rate, and decrease bucket size to reduce variance. We will not quantize small gradient matrices ($< 10K$ elements), since the computational cost of quantizing them significantly exceeds the reduction in communication. However, in all experiments, more than 99% of all parameters are transmitted in quantized form. We reshape matrices to fit bucket sizes, so that no receptive field is split across two buckets.

Communication vs. Computation. In the first set of experiments, we examine the ratio between computation and communication costs during training, for increased parallelism. The image classification networks are trained on ImageNet, while LSTM is trained on AN4. We examine the cost breakdown for these networks over a pass over the dataset (epoch). Figure 2 gives the results for various networks for image classification. The variance of epoch times is practically negligible ($< 1\%$), hence we omit confidence intervals.

Figure 2 leads to some interesting observations. First, based on the ratio of communication to computation, we can roughly split networks into *communication-intensive* (AlexNet, VGG, LSTM), and *computation-intensive* (Inception, ResNet). For both network types, the relative impact of communication *increases significantly* as we increase the number of GPUs. Examining the breakdown for the 32-bit version, all networks could significantly benefit from reduced communication. For

example, for AlexNet on 16 GPUs with batch size 1024, more than 80% of training time is spent on communication, whereas for LSTM on 2 GPUs with batch size 256, the ratio is 71%. (These ratios can be slightly changed by increasing batch size, but this can decrease accuracy, see e.g. [21].)

Next, we examine the impact of QSGD on communication and overall training time. (Communication time includes time spent compressing and uncompressing gradients.) We measured QSGD with 2-bit quantization and 128 bucket size, and 4-bit and 8-bit quantization with 512 bucket size. The results for these two variants are similar, since the different bucket sizes mean that the 4bit version only sends 77% more data than the 2-bit version (but $\sim 8\times$ less than 32-bit). These bucket sizes are chosen to ensure good convergence, but are not carefully tuned.

On 16GPU AlexNet with batch size 1024, 4-bit QSGD reduces communication time by $4\times$, and overall epoch time by $2.5\times$. On LSTM, it reduces communication time by $6.8\times$, and overall epoch time by $2.7\times$. Runtime improvements are non-trivial for all architectures we considered.

Accuracy. We now examine how QSGD influences accuracy and convergence rate. We ran AlexNet and ResNet to full convergence on ImageNet, LSTM on AN4, ResNet110 on CIFAR-10, as well as a two-layer perceptron on MNIST. Results are given in Figure 5, and exact numbers are given in Table 1. QSGD tests are performed on an 8GPU setup, and are compared against the best known full-precision accuracy of the networks. In general, we notice that 4bit or 8bit gradient quantization is sufficient to recover or even slightly improve full accuracy, while ensuring non-trivial speedup. Across all our experiments, 8-bit gradients with 512 bucket size have been sufficient to recover or improve upon the full-precision accuracy. Our results are consistent with recent work [30] noting benefits of adding noise to gradients when training deep networks. Thus, quantization can be seen as a source of zero-mean noise, which happens to render communication more efficient. At the same time, we note that more aggressive quantization can hurt accuracy. In particular, 4-bit QSGD with 8192 bucket size (not shown) loses 0.57% for top-5 accuracy, and 0.68% for top-1, versus full precision on AlexNet when trained for the same number of epochs. Also, QSGD with 2-bit and 64 bucket size has gap 1.73% for top-1, and 1.18% for top-1.

One issue we examined in more detail is which layers are more sensitive to quantization. It appears that quantizing *convolutional layers* too aggressively (e.g., 2-bit precision) can lead to accuracy loss if trained for the same period of time as the full precision variant. However, increasing precision to 4-bit or 8-bit recovers accuracy. This finding suggests that modern architectures for vision tasks, such as ResNet or Inception, which are almost entirely convolutional, may benefit less from quantization than recurrent deep networks such as LSTMs.

Additional Experiments. The full version of the paper contains additional experiments, including a full comparison with 1BitSGD. In brief, QSGD outperforms or matches the performance and final accuracy of 1BitSGD for the networks and parameter values we consider.

6 Conclusions and Future Work

We have presented QSGD, a family of SGD algorithms which allow a smooth trade off between the amount of communication per iteration and the running time. Experiments suggest that QSGD is highly competitive with the full-precision variant on a variety of tasks. There are a number of optimizations we did not explore. The most significant is leveraging the *sparsity* created by QSGD. Current implementations of MPI do not provide support for sparse types, but we plan to explore such support in future work. Further, we plan to examine the potential of QSGD in larger-scale applications, such as super-computing. On the theoretical side, it is interesting to consider applications of quantization beyond SGD.

The full version of this paper [4] contains complete proofs, as well as additional applications.

7 Acknowledgments

The authors would like to thank Martin Jaggi, Ce Zhang, Frank Seide and the CNTK team for their support during the development of this project, as well as the anonymous NIPS reviewers for their careful consideration and excellent suggestions. Dan Alistarh was supported by a Swiss National Fund Ambizione Fellowship. Jerry Li was supported by the NSF CAREER Award CCF-1453261, CCF-1565235, a Google Faculty Research Award, and an NSF Graduate Research Fellowship. This work was developed in part while Dan Alistarh, Jerri Li and Milan Vojnovic were with Microsoft Research Cambridge, UK.

References

- [1] Martin Abadi, Ashish Agarwal, Paul Barham, Eugene Brevdo, Zhifeng Chen, Craig Citro, Greg S Corrado, Andy Davis, Jeffrey Dean, Matthieu Devin, et al. Tensorflow: Large-scale machine learning on heterogeneous distributed systems. *arXiv preprint arXiv:1603.04467*, 2016.
- [2] Alex Acero. *Acoustical and environmental robustness in automatic speech recognition*, volume 201. Springer Science & Business Media, 2012.
- [3] Amit Agarwal, Eldar Akchurin, Chris Basoglu, Guoguo Chen, Scott Cyphers, Jasha Droppo, Adam Eversole, Brian Guenter, Mark Hillebrand, Ryan Hoens, et al. An introduction to computational networks and the computational network toolkit. Technical report, Tech. Rep. MSR-TR-2014-112, August 2014., 2014.
- [4] Dan Alistarh, Demjan Grubic, Jerry Li, Ryota Tomioka, and Milan Vojnovic. QSGD: Communication-efficient SGD via gradient quantization and encoding. *arXiv preprint arXiv:1610.02132*, 2016.
- [5] Yossi Arjevani and Ohad Shamir. Communication complexity of distributed convex learning and optimization. In *NIPS*, 2015.
- [6] Ron Bekkerman, Mikhail Bilenko, and John Langford. *Scaling up machine learning: Parallel and distributed approaches*. Cambridge University Press, 2011.
- [7] Sébastien Bubeck. Convex optimization: Algorithms and complexity. *Foundations and Trends® in Machine Learning*, 8(3-4):231–357, 2015.
- [8] Trishul Chilimbi, Yutaka Suzue, Johnson Apacible, and Karthik Kalyanaraman. Project adam: Building an efficient and scalable deep learning training system. In *OSDI*, October 2014.
- [9] Cntk brainscript file for alexnet. <https://github.com/Microsoft/CNTK/tree/master/Examples/Image/Classification/AlexNet/BrainScript>. Accessed: 2017-02-24.
- [10] Christopher M De Sa, Ce Zhang, Kunle Olukotun, and Christopher Ré. Taming the wild: A unified analysis of hogwild-style algorithms. In *NIPS*, 2015.
- [11] Jeffrey Dean, Greg Corrado, Rajat Monga, Kai Chen, Matthieu Devin, Mark Mao, Andrew Senior, Paul Tucker, Ke Yang, Quoc V Le, et al. Large scale distributed deep networks. In *NIPS*, 2012.
- [12] Jia Deng, Wei Dong, Richard Socher, Li-Jia Li, Kai Li, and Li Fei-Fei. Imagenet: A large-scale hierarchical image database. In *Computer Vision and Pattern Recognition, 2009. CVPR 2009. IEEE Conference on*, pages 248–255. IEEE, 2009.
- [13] John C Duchi, Sorathan Chaturapruek, and Christopher Ré. Asynchronous stochastic convex optimization. *NIPS*, 2015.
- [14] Peter Elias. Universal codeword sets and representations of the integers. *IEEE transactions on information theory*, 21(2):194–203, 1975.
- [15] Saeed Ghadimi and Guanghui Lan. Stochastic first- and zeroth-order methods for nonconvex stochastic programming. *SIAM Journal on Optimization*, 23(4):2341–2368, 2013.
- [16] Suyog Gupta, Ankur Agrawal, Kailash Gopalakrishnan, and Pritish Narayanan. Deep learning with limited numerical precision. In *ICML*, pages 1737–1746, 2015.
- [17] Song Han, Huizi Mao, and William J Dally. Deep compression: Compressing deep neural networks with pruning, trained quantization and huffman coding. *arXiv preprint arXiv:1510.00149*, 2015.
- [18] Kaiming He, Xiangyu Zhang, Shaoqing Ren, and Jian Sun. Deep residual learning for image recognition. In *Proceedings of the IEEE Conference on Computer Vision and Pattern Recognition*, pages 770–778, 2016.
- [19] Sepp Hochreiter and Jürgen Schmidhuber. Long short-term memory. *Neural computation*, 9(8):1735–1780, 1997.
- [20] Itay Hubara, Matthieu Courbariaux, Daniel Soudry, Ran El-Yaniv, and Yoshua Bengio. Binarized neural networks. In *Advances in Neural Information Processing Systems*, pages 4107–4115, 2016.

- [21] Forrest N Iandola, Matthew W Moskewicz, Khalid Ashraf, and Kurt Keutzer. Firecaffe: near-linear acceleration of deep neural network training on compute clusters. In *Proceedings of the IEEE Conference on Computer Vision and Pattern Recognition*, pages 2592–2600, 2016.
- [22] Sergey Ioffe and Christian Szegedy. Batch normalization: Accelerating deep network training by reducing internal covariate shift. *arXiv preprint arXiv:1502.03167*, 2015.
- [23] Rie Johnson and Tong Zhang. Accelerating stochastic gradient descent using predictive variance reduction. In *NIPS*, 2013.
- [24] Jakub Konečný. Stochastic, distributed and federated optimization for machine learning. *arXiv preprint arXiv:1707.01155*, 2017.
- [25] Alex Krizhevsky and Geoffrey Hinton. Learning multiple layers of features from tiny images, 2009.
- [26] Alex Krizhevsky, Ilya Sutskever, and Geoffrey E Hinton. Imagenet classification with deep convolutional neural networks. In *Advances in neural information processing systems*, pages 1097–1105, 2012.
- [27] Yann LeCun, Corinna Cortes, and Christopher JC Burges. The mnist database of handwritten digits, 1998.
- [28] Mu Li, David G Andersen, Jun Woo Park, Alexander J Smola, Amr Ahmed, Vanja Josifovski, James Long, Eugene J Shekita, and Bor-Yiing Su. Scaling distributed machine learning with the parameter server. In *OSDI*, 2014.
- [29] Xiangru Lian, Yijun Huang, Yuncheng Li, and Ji Liu. Asynchronous parallel stochastic gradient for nonconvex optimization. In *NIPS*. 2015.
- [30] Arvind Neelakantan, Luke Vilnis, Quoc V Le, Ilya Sutskever, Lukasz Kaiser, Karol Kurach, and James Martens. Adding gradient noise improves learning for very deep networks. *arXiv preprint arXiv:1511.06807*, 2015.
- [31] Cntk implementation of qsgd. <https://gitlab.com/demjanrubic/QSGD>. Accessed: 2017-11-4.
- [32] Benjamin Recht, Christopher Re, Stephen Wright, and Feng Niu. Hogwild: A lock-free approach to parallelizing stochastic gradient descent. In *NIPS*, 2011.
- [33] Herbert Robbins and Sutton Monro. A stochastic approximation method. *The Annals of Mathematical Statistics*, pages 400–407, 1951.
- [34] Richard Schreier and Gabor C Temes. *Understanding delta-sigma data converters*, volume 74. IEEE Press, Piscataway, NJ, 2005.
- [35] Frank Seide, Hao Fu, Jasha Droppo, Gang Li, and Dong Yu. 1-bit stochastic gradient descent and its application to data-parallel distributed training of speech dnns. In *INTERSPEECH*, 2014.
- [36] Karen Simonyan and Andrew Zisserman. Very deep convolutional networks for large-scale image recognition. *arXiv preprint arXiv:1409.1556*, 2014.
- [37] Nikko Strom. Scalable distributed DNN training using commodity GPU cloud computing. In *INTERSPEECH*, 2015.
- [38] Ananda Theertha Suresh, Felix X Yu, H Brendan McMahan, and Sanjiv Kumar. Distributed mean estimation with limited communication. *arXiv preprint arXiv:1611.00429*, 2016.
- [39] Seiya Tokui, Kenta Oono, Shohei Hido, CA San Mateo, and Justin Clayton. Chainer: a next-generation open source framework for deep learning. In *Proceedings of workshop on machine learning systems (LearningSys)*, 2015.
- [40] John N Tsitsiklis and Zhi-Quan Luo. Communication complexity of convex optimization. *Journal of Complexity*, 3(3), 1987.
- [41] Wei Wen, Cong Xu, Feng Yan, Chunpeng Wu, Yandan Wang, Yiran Chen, and Hai Li. Terngrad: Ternary gradients to reduce communication in distributed deep learning. *arXiv preprint arXiv:1705.07878*, 2017.
- [42] Hantian Zhang, Jerry Li, Kaan Kara, Dan Alistarh, Ji Liu, and Ce Zhang. Zipml: Training linear models with end-to-end low precision, and a little bit of deep learning. In *International Conference on Machine Learning*, pages 4035–4043, 2017.

- [43] Sixin Zhang, Anna E Choromanska, and Yann LeCun. Deep learning with elastic averaging SGD. In *Advances in Neural Information Processing Systems*, pages 685–693, 2015.
- [44] Yuchen Zhang, John Duchi, Michael I Jordan, and Martin J Wainwright. Information-theoretic lower bounds for distributed statistical estimation with communication constraints. In *NIPS*, 2013.
- [45] Shuchang Zhou, Yuxin Wu, Zekun Ni, Xinyu Zhou, He Wen, and Yuheng Zou. Dorefa-net: Training low bitwidth convolutional neural networks with low bitwidth gradients. *arXiv preprint arXiv:1606.06160*, 2016.

Roadmap of the Appendix

A Proof of Lemmas and Theorems

A.1 Proof of Lemma 3.1

The first claim obviously holds. We thus turn our attention to the second claim of the lemma. We first note the following bound:

$$\begin{aligned}
\mathbb{E}[\xi_i(\mathbf{v}, s)^2] &= \mathbb{E}[\xi_i(\mathbf{v}, s)]^2 + \mathbb{E}\left[\left(\xi_i(\mathbf{v}, s) - \mathbb{E}[\xi_i(\mathbf{v}, s)]\right)^2\right] \\
&= \frac{v_i^2}{\|\mathbf{v}\|_2^2} + \frac{1}{s^2}p\left(\frac{|v_i|}{\|\mathbf{v}\|_2}, s\right)\left(1 - p\left(\frac{|v_i|}{\|\mathbf{v}\|_2}, s\right)\right) \\
&\leq \frac{v_i^2}{\|\mathbf{v}\|_2^2} + \frac{1}{s^2}p\left(\frac{|v_i|}{\|\mathbf{v}\|_2}, s\right).
\end{aligned}$$

Using this bound, we have

$$\begin{aligned}
\mathbb{E}[\|Q(\mathbf{v}, s)\|^2] &= \sum_{i=1}^n \mathbb{E}\left[\|\mathbf{v}\|_2^2 \xi_i\left(\frac{|v_i|}{\|\mathbf{v}\|_2}, s\right)^2\right] \\
&\leq \|\mathbf{v}\|_2^2 \sum_{i=1}^n \left[\frac{|v_i|^2}{\|\mathbf{v}\|_2^2} + \frac{1}{s^2}p\left(\frac{|v_i|}{\|\mathbf{v}\|_2}, s\right)\right] \\
&= \left(1 + \frac{1}{s^2} \sum_{i=1}^n p\left(\frac{|v_i|}{\|\mathbf{v}\|_2}, s\right)\right) \|\mathbf{v}\|_2^2 \\
&\stackrel{a}{\leq} \left(1 + \min\left(\frac{n}{s^2}, \frac{\|\mathbf{v}\|_1}{s\|\mathbf{v}\|_2}\right)\right) \|\mathbf{v}\|_2^2 \\
&\leq \left(1 + \min\left(\frac{n}{s^2}, \frac{\sqrt{n}}{s}\right)\right) \|\mathbf{v}\|_2^2.
\end{aligned}$$

where (a) follows from the fact that $p(a, s) \leq 1$ and $p(a, s) \leq as$. This immediately implies that $\mathbb{E}[\|Q(\mathbf{v}, s) - \mathbf{v}\|_2^2] \leq \min\left(\frac{n}{s^2}, \frac{\sqrt{n}}{s}\right) \cdot \|\mathbf{v}\|_2^2$, as claimed.

A.2 A Compression Scheme for Q_s Matching Theorem 3.2

In this section, we describe a scheme for coding Q_s and provide an upper bound for the expected number of information bits that it uses, which gives the bound in Theorem 3.2.

Observe that for any vector \mathbf{v} , the output of $Q(\mathbf{v}, s)$ is naturally expressible by a tuple $(\|\mathbf{v}\|_2, \boldsymbol{\sigma}, \boldsymbol{\zeta})$, where $\boldsymbol{\sigma}$ is the vector of signs of the v_i 's and $\boldsymbol{\zeta}$ is the vector of $\xi_i(\mathbf{v}, s)$ values. With a slight abuse of notation, let us consider $Q(\mathbf{v}, s)$ as a function from $\mathbb{R} \setminus \{0\}$ to \mathcal{B}_s , where

$$\mathcal{B}_s = \{(A, \boldsymbol{\sigma}, \mathbf{z}) \in \mathbb{R} \times \mathbb{R}^n \times \mathbb{R}^n : A \in \mathbb{R}_{\geq 0}, \boldsymbol{\sigma}_i \in \{-1, +1\}, \mathbf{z}_i \in \{0, 1/s, \dots, 1\}\}.$$

We define a coding scheme that represents each tuple in \mathcal{B}_s with a codeword in $\{0, 1\}^*$ according to a mapping $\text{Code}_s : \mathcal{B}_s \rightarrow \{0, 1\}^*$.

To encode a single coordinate, we utilize a lossless encoding scheme for positive integers known as *recursive Elias coding* or *Elias omega coding*.

Definition A.1. Let k be a positive integer. The *recursive Elias coding* of k , denoted $\text{Elias}(k)$, is defined to be the $\{0, 1\}$ string constructed as follows. First, place a 0 at the end of the string. If $k = 0$, then terminate. Otherwise, prepend the binary representation of k to the beginning of the code. Let k' be the number of bits so prepended minus 1, and recursively encode k' in the same fashion. To decode an recursive Elias coded integer, start with $N = 1$. Recursively, if the next bit is 0, stop, and output N . Otherwise, if the next bit is 1, then read that bit and N additional bits, and let that number in binary be the new N , and repeat.

The following are well-known properties of the recursive Elias code which are not too hard to prove.

Lemma A.1. For any positive integer k , we have

1. $|\text{Elias}(k)| \leq \log k + \log \log k + \log \log \log k \dots + 1 = (1 + o(1)) \log k + 1$.
2. The recursive Elias code of k can be encoded and decoded in time $O(|\text{Elias}(k)|)$.
3. Moreover, the decoding can be done without previously knowing a bound on the size of k .

Given a tuple $(A, \sigma, z) \in \mathcal{B}_s$, our coding outputs a string S defined as follows. First, it uses F bits to encode A . It proceeds to encode using Elias recursive coding the position of the first nonzero entry of z . It then appends a bit denoting σ_i and follows that with $\text{Elias}(sz_i)$. Iteratively, it proceeds to encode the distance from the current coordinate of z to the next nonzero using c , and encodes the σ_i and z_i for that coordinate in the same way. The decoding scheme is also straightforward: we first read off F bits to construct A , then iteratively use the decoding scheme for Elias recursive coding to read off the positions and values of the nonzeros of z and σ .

We can now present a full description of our lossy-compression scheme. For any input vector \mathbf{v} , we first compute quantization $Q(\mathbf{v}, s)$, and then encode using Code_s . In our notation, this is expressed as $\mathbf{v} \rightarrow \text{Code}_s(Q(\mathbf{v}, s))$.

Lemma A.2. For any $\mathbf{v} \in \mathbb{R}^n$ and $s^2 + \sqrt{n} \leq n/2$, we have

$$\mathbb{E}[|\text{Code}_s(Q(\mathbf{v}, s))|] \leq \left(3 + \frac{3}{2} \cdot (1 + o(1)) \log \left(\frac{2(s^2 + n)}{s^2 + \sqrt{n}} \right)\right) (s^2 + \sqrt{n}).$$

This lemma together with Lemma 3.1 suffices to prove Theorem 3.2.

We first show a technical lemma about the behavior of the coordinate-wise coding function c on a vector with bounded ℓ_p norm.

Lemma A.3. Let $\mathbf{q} \in \mathbb{R}^d$ be a vector so that for all i , we have that q_i is a positive integer, and moreover, $\|\mathbf{q}\|_p^p \leq \rho$. Then

$$\sum_{i=1}^d |\text{Elias}(\mathbf{q}_i)| \leq \left(\frac{1 + o(1)}{p} \log \left(\frac{\rho}{n} \right) + 1 \right) n.$$

Proof. Recall that for any positive integer k , the length of $\text{Elias}(k)$ is at most $(1 + o(1)) \log k + 1$. Hence, we have

$$\begin{aligned} \sum_{i=1}^d |\text{Elias}(\mathbf{q}_i)| &\leq (1 + o(1)) \sum_{i=1}^d (\log \mathbf{q}_i) + d \\ &\leq \frac{1 + o(1)}{p} \sum_{i=1}^n (\log(\mathbf{q}_i^p)) + d \\ &\stackrel{(a)}{\leq} \frac{1 + o(1)}{p} n \log \left(\frac{1}{n} \sum_{i=1}^n \mathbf{q}_i^p \right) + d \\ &\leq \frac{1 + o(1)}{p} n \log \left(\frac{\rho}{n} \right) + n \end{aligned}$$

where (a) follows from Jensen's inequality. \square

We can bound the number of information bits needed for our coding scheme in terms of the number of non-zeroes of our vector.

Lemma A.4. *For any tuple $(A, \boldsymbol{\sigma}, \mathbf{z}) \in \mathcal{B}_s$, the string $\text{Code}_s(A, \boldsymbol{\sigma}, \mathbf{z})$ has length of at most this many bits:*

$$F + \left((1 + o(1)) \cdot \log \left(\frac{n}{\|\mathbf{z}\|_0} \right) + \frac{1 + o(1)}{2} \log \left(\frac{s^2 \|\mathbf{z}\|_2^2}{\|\mathbf{z}\|_0} + 3 \right) \right) \cdot \|\mathbf{z}\|_0.$$

Proof. First, the float A takes F bits to communicate. Let us now consider the rest of the string. We break up the string into a couple of parts. First, there is the subsequence S_1 dedicated to pointing to the next nonzero coordinate of \mathbf{z} . Second, there is the subsequence S_2 dedicated to communicating the sign and $c(z_i)$ for each nonzero coordinate i . While these two sets of bits are not consecutive within the string, it is clear that they partition the remaining bits in the string. We bound the length of these two substrings separately.

We first bound the length of S_1 . Let $i_1, \dots, i_{\|\mathbf{z}\|_0}$ be the nonzero coordinates of \mathbf{z} . Then, from the definition of Code_s , it is not hard to see that S_1 consists of the encoding of the vector

$$\mathbf{q}^{(1)} = (i_1, i_2 - i_1, \dots, i_{\|\mathbf{z}\|_0} - i_{\|\mathbf{z}\|_0 - 1}),$$

where each coordinate of this vector is encoded using c . By Lemma A.3, since this vector has length $\|\mathbf{z}\|_0$ and has ℓ_1 norm at most n , we have that

$$|S_1| \leq \left((1 + o(1)) \log \frac{n}{\|\mathbf{z}\|_0} + 1 \right) \|\mathbf{z}\|_0. \quad (5)$$

We now bound the length of S_2 . Per non-zero coordinate of \mathbf{z} , we need to communicate a sign (which takes one bit), and $c(s z_i)$. Thus by Lemma A.3, we have that

$$\begin{aligned} |S_2| &= \sum_{j=1}^{\|\mathbf{z}\|_0} (1 + |\text{Elias}(s z_i)|) \\ &\leq \|\mathbf{z}\|_0 + \left(\frac{(1 + o(1))}{2} \log \frac{s^2 \|\mathbf{z}\|_2^2}{\|\mathbf{z}\|_0} + 1 \right) \|\mathbf{z}\|_0. \end{aligned} \quad (6)$$

Putting together (5) and (6) yields the desired conclusion. \square

We first need the following technical lemma about the number of nonzeros of $Q(\mathbf{v}, s)$ that we have in expectation.

Lemma A.5. *Let $\mathbf{v} \in \mathbb{R}^n$ such that $\|\mathbf{v}\|_2 \neq 0$. Then*

$$\mathbb{E}[\|Q(\mathbf{v}, s)\|_0] \leq s^2 + \sqrt{n}.$$

Proof. Let $\mathbf{u} = \mathbf{v}/\|\mathbf{v}\|_2$. Let $I(\mathbf{u})$ denote the set of coordinates i of \mathbf{u} so that $u_i \leq 1/s$. Since

$$1 \geq \sum_{i \notin I(\mathbf{u})} u_i^2 \geq (n - |I(\mathbf{u})|)/s^2,$$

we must have that $s^2 \geq n - |I(\mathbf{u})|$. Moreover, for each $i \in I(\mathbf{u})$, we have that $Q_i(\mathbf{v}, s)$ is nonzero with probability u_i , and zero otherwise. Hence

$$\mathbb{E}[L(\mathbf{v})] \leq n - |I(\mathbf{u})| + \sum_{i \in I(\mathbf{u})} u_i \leq s^2 + \|\mathbf{u}\|_1 \leq s^2 + \sqrt{n}.$$

\square

Proof of Lemma A.2 Let $Q(\mathbf{v}, s) = (\|\mathbf{v}\|_2, \boldsymbol{\sigma}, \boldsymbol{\zeta})$, and let $\mathbf{u} = \mathbf{v}/\|\mathbf{v}\|_2$. Observe that we always have that

$$\|\boldsymbol{\zeta}\|_2^2 \leq \sum_{i=1}^n \left(u_i + \frac{1}{s}\right)^2 \stackrel{(a)}{\leq} 2 \sum_{i=1}^n u_i^2 + 2 \sum_{i=1}^n \frac{1}{s^2} = 2 \left(1 + \frac{n}{s^2}\right), \quad (7)$$

where (a) follows since $(a+b)^2 \leq 2(a^2 + b^2)$ for all $a, b \in \mathbb{R}$.

By Lemma A.4, we now have that

$$\begin{aligned} \mathbb{E}[|\text{Code}_s(Q(\mathbf{v}, s))|] &\leq F + (1 + o(1)) \mathbb{E} \left[\|\boldsymbol{\zeta}\|_0 \log \left(\frac{n}{\|\boldsymbol{\zeta}\|_0} \right) \right] \\ &\quad + \frac{1 + o(1)}{2} \mathbb{E} \left[\|\boldsymbol{\zeta}\|_0 \log \left(\frac{s^2 R(\boldsymbol{\zeta})}{\|\boldsymbol{\zeta}\|_0} \right) \right] + 3 \mathbb{E}[\|\boldsymbol{\zeta}\|_0] \\ &\leq F + (1 + o(1)) \mathbb{E} \left[\|\boldsymbol{\zeta}\|_0 \log \left(\frac{n}{\|\boldsymbol{\zeta}\|_0} \right) \right] + \\ &\quad \frac{1 + o(1)}{2} \mathbb{E} \left[\|\boldsymbol{\zeta}\|_0 \log \left(\frac{2(s^2 + n)}{\|\boldsymbol{\zeta}\|_0} \right) \right] + 3(s^2 + \sqrt{n}), \end{aligned}$$

by (7) and Lemma A.5.

It is a straightforward verification that the function $f(x) = x \log \left(\frac{C}{x} \right)$ is concave for all $C > 0$. Moreover, it is increasing up until $x = C/2$, and decreasing afterwards. Hence, by Jensen's inequality, Lemma A.5, and the assumption that $s^2 + \sqrt{n} \leq n/2$, we have that

$$\begin{aligned} \mathbb{E} \left[\|\boldsymbol{\zeta}\|_0 \log \left(\frac{n}{\|\boldsymbol{\zeta}\|_0} \right) \right] &\leq (s^2 + \sqrt{n}) \log \left(\frac{n}{s^2 + \sqrt{n}} \right), \text{ and} \\ \mathbb{E} \left[\|\boldsymbol{\zeta}\|_0 \log \left(\frac{2(s^2 + n)}{\|\boldsymbol{\zeta}\|_0} \right) \right] &\leq (s^2 + \sqrt{n}) \log \left(\frac{2(s^2 + n)}{s^2 + \sqrt{n}} \right). \end{aligned}$$

Simplifying yields the expression in the Lemma.

A.3 A Compression Scheme for Q_s Matching Theorem 3.3

For the case of the quantized SGD scheme that requires $\Theta(n)$ bits per iteration, we can improve the constant factor in the bit length bound in Theorem A.2 by using a different encoding of $Q(\mathbf{v}, s)$. This corresponds to the regime where $s = \sqrt{n}$, i.e., where the quantized update is not expected to be sparse. In this case, there is no advantage gained by transmitting the location of the next nonzero, since generally that will simply be the next coordinate of the vector. Therefore, we may as well simply transmit the value of each coordinate in sequence.

Motivated by the above remark, we define the following alternative compression function. Define $\text{Elias}'(k) = \text{Elias}(k+1)$ to be a compression function on all nonnegative natural numbers. It is easy to see that this is uniquely decodable. Let Code'_s be the compression function which, on input $(A, \boldsymbol{\sigma}, \mathbf{z})$, simply encodes every coordinate of \mathbf{z} in the same way as before, even if it is zero, using Elias' . It is straightforward to show that this compression function is still uniquely decodable. Then, just as before, our full quantization scheme is as follows. For any arbitrary vector \mathbf{v} , we first compute $Q(\mathbf{v}, s)$, and then encode using Code'_s . In our notation, this is expressed as $\mathbf{v} \rightarrow \text{Code}'_s(Q(\mathbf{v}, s))$. For this compression scheme, we show:

Lemma A.6. *For any $\mathbf{v} \in \mathbb{R}^n$, we have*

$$\mathbb{E}[|\text{Code}'_s(Q(\mathbf{v}, s))|] \leq F + \left(\frac{1 + o(1)}{2} \left(\log \left(1 + \frac{s^2 + \min(n, s\sqrt{n})}{n} \right) + 1 \right) + 2 \right) n.$$

In particular, if $s = \sqrt{n}$, then $\mathbb{E}[|\text{Code}'_s(Q(\mathbf{v}, s))|] \leq F + 2.8n$.

It is not hard to see that this is equivalent to the bound stated in Theorem 3.3.

We start by showing the following lemma.

Lemma A.7. For any tuple $(A, \boldsymbol{\sigma}, \mathbf{z}) \in \mathcal{B}_s$, the string $\text{Code}'_s(A, \boldsymbol{\sigma}, \mathbf{z})$ has length of at most this many bits:

$$F + \left(\frac{1 + o(1)}{2} \left(\log \left(1 + \frac{s^2 \|\mathbf{z}\|_2^2}{n} \right) + 1 \right) + 2 \right) n.$$

Proof. The proof of this lemma follows by similar arguments as that of Lemma A.4. The main differences are that (1) we do not need to encode the position of the nonzeros, and (2) we always encode $\text{Elias}(k+1)$ instead of $\text{Elias}(k)$. Hence, for coordinate i , we require $1 + \text{Elias}(s\mathbf{z}_i + 1)$ bits, since in addition to encoding \mathbf{z}_i we must also encode the sign. Thus the total number of bits may be bounded by

$$\begin{aligned} F + \sum_{i=1}^n (\text{Elias}(\mathbf{z}_i + 1) + 1) &= F + n + \sum_{i=1}^n \text{Elias}(s\mathbf{z}_i + 1) \\ &\leq F + n + \sum_{i=1}^n [(1 + o(1)) \log(s\mathbf{z}_i + 1) + 1] \\ &\leq F + 2n + (1 + o(1)) \sum_{i=1}^n \log(s\mathbf{z}_i + 1) \\ &\leq F + 2n + \frac{1 + o(1)}{2} \sum_{i=1}^n \log((s\mathbf{z}_i + 1)^2) \\ &\stackrel{(a)}{\leq} F + 2n + \frac{1 + o(1)}{2} \sum_{i=1}^n (\log(1 + s^2 \mathbf{z}_i^2) + \log(2)) \\ &\stackrel{(b)}{\leq} F + 2n + \frac{1 + o(1)}{2} n \left(\log \left(1 + \frac{1}{n} \sum_{i=1}^n s^2 \mathbf{z}_i^2 \right) + 1 \right) \end{aligned}$$

where (a) follows from basic properties of logarithms and (b) follows from the concavity of the function $x \mapsto \log(1 + x)$ and Jensen's inequality. Simplifying yields the desired statement. \square

Proof of Lemma A.6 As in the proof of Lemma A.2, let $Q(\mathbf{v}, s) = (\|\mathbf{v}\|_2, \boldsymbol{\sigma}, \boldsymbol{\zeta})$, and let $\mathbf{u} = \mathbf{v}/\|\mathbf{v}\|_2$. By Lemma A.7, we have

$$\begin{aligned} \mathbb{E}[\|\text{Code}'_s(Q(\mathbf{v}, s))\|] &\leq F + \left(\frac{1 + o(1)}{2} \left(\mathbb{E} \left[\log \left(1 + \frac{s^2 R(\boldsymbol{\zeta})}{n} \right) \right] + 1 \right) + 2 \right) n \\ &\stackrel{(a)}{\leq} F + \left(\frac{1 + o(1)}{2} \left(\log \left(1 + \frac{\mathbb{E}[s^2 R(\boldsymbol{\zeta})]}{n} \right) + 1 \right) + 2 \right) n \\ &\stackrel{(b)}{\leq} F + \left(\frac{1 + o(1)}{2} \left(\log \left(1 + \frac{s^2(1 + \min(n/s^2, \sqrt{n}/s))}{n} \right) + 1 \right) + 2 \right) n \end{aligned}$$

where (a) follows from Jensen's inequality, and (b) follows from the proof of Lemma 3.1.

B Quantized SVRG

Variance Reduction for Sums of Smooth Functions. One common setting in which SGD sees application in machine learning is when f can be naturally expressed as a sum of smooth functions. Formally, we assume that $f(\mathbf{x}) = \frac{1}{m} \sum_{i=1}^m f_i(\mathbf{x})$. When f can be expressed as a sum of smooth functions, this lends itself naturally to SGD. This is because a natural stochastic gradient for f in this setting is, on input \mathbf{x} , to sample a uniformly random index i , and output $\nabla f_i(\mathbf{x})$. We will also impose somewhat stronger assumptions on f and f_1, f_2, \dots, f_m , namely, that f is strongly convex, and that each f_i is convex and smooth.

Definition B.1 (Strong Convexity). Let $f : \mathbb{R}^n \rightarrow \mathbb{R}$ be a differentiable function. We say that f is ℓ -strongly convex if for all $x, y \in \mathbb{R}^n$, we have

$$f(x) - f(y) \leq \nabla f(x)^T(x - y) - \frac{\ell}{2}\|x - y\|_2^2.$$

Observe that when $\ell = 0$ this is the standard definition of convexity.

Note that it is well-known that even if we impose these stronger assumptions on f and f_1, f_2, \dots, f_m , then by only applying SGD one still cannot achieve exponential convergence rates, i.e. error rates which improve as $\exp(-T)$ at iteration T . (Such a rate is known in the optimization literature as *linear* convergence.) However, an epoch-based modification of SGD, known as stochastic variance reduced gradient descent (SVRG) [23], is able to give such rates in this specific setting. We describe the method below, following the presentation of Bubeck [7].

Background on SVRG. Let $\mathbf{y}^{(1)} \in \mathbb{R}^n$ be an arbitrary point. For $p = 1, 2, \dots, P$, we let $\mathbf{x}_1^{(p)} = \mathbf{y}^{(p)}$. Each p is called an *epoch*. Then, within epoch p , for $t = 1, \dots, T$, we let $i_t^{(p)}$ be a uniformly random integer from $[m]$ completely independent from everything else, and we set:

$$\mathbf{x}_{t+1}^{(p)} = \mathbf{x}_t^{(p)} - \eta \left(\nabla f_{i_t^{(p)}}(\mathbf{x}_t^{(p)}) - \nabla f_{i_t^{(p)}}(\mathbf{y}^{(p)}) + \nabla f(\mathbf{y}^{(p)}) \right).$$

We then set

$$\mathbf{y}^{(p+1)} = \frac{1}{k} \sum_{i=1}^k \mathbf{x}_i^{(p)}.$$

With this iterative scheme, we have the following guarantee:

Theorem B.1 ([23]). Let $f(\mathbf{x}) = \frac{1}{m} \sum_{i=1}^m f_i(\mathbf{x})$, where f is ℓ -strongly convex, and f_i are convex and L -smooth, for all i . Let \mathbf{x}^* be the unique minimizer of f over \mathbb{R}^n . Then, if $\eta = O(1/L)$ and $T = O(L/\ell)$, we have

$$\mathbb{E} \left[f(\mathbf{y}^{(p+1)}) \right] - f(\mathbf{x}^*) \leq 0.9^p \left(f(\mathbf{y}^{(1)}) - f(\mathbf{x}^*) \right). \quad (8)$$

Quantized SVRG. In parallel SVRG, we are given K processors, each processor i having access to $f_{im/K}, \dots, f_{(i+1)m/K-1}$. The goal is the same as before: to approximately minimize $f = \frac{1}{m} \sum_{i=1}^m f_i$. For processor i , let $h_i = \frac{1}{m} \sum_{j=im/K}^{(i+1)m/K-1} f_j$ be the portion of f that it knows, so that $f = \sum_{i=1}^K h_i$.

A natural question is whether we can apply randomized quantization to reduce communication for parallel SVRG. Whenever one applies our quantization functions to the gradient updates in SVRG, the resulting update is no longer an update of the form used in SVRG, and hence the analysis for SVRG does not immediately give any results in black-box fashion. Instead, we prove that despite this technical issue, one can quantize SVRG updates using our techniques and still obtain the same convergence bounds.

Let $\tilde{Q}(\mathbf{v}) = Q(\mathbf{v}, \sqrt{n})$, where $Q(\mathbf{v}, s)$ is defined as in Section 3.1. Our quantized SVRG updates are as follows. Given arbitrary starting point \mathbf{x}_0 , we let $\mathbf{y}^{(1)} = \mathbf{x}_0$. At the beginning of epoch p , each processor broadcasts

$$H_{p,i} = \tilde{Q} \left(\frac{1}{m} \sum_{j=im/K}^{(i+1)m/K-1} \nabla f_j(\mathbf{y}^{(p)}) \right) = \tilde{Q}(\nabla h_i),$$

from which the processors collectively form $H_p = \sum_{i=1}^m H_{p,i}$ without additional communication. Within each epoch, for each iteration $t = 1, \dots, T$, and for each processor $i = 1, \dots, K$, we let $j_{i,t}^{(p)}$ be a uniformly random integer from $[m]$ completely independent from everything else. Then, in iteration t in epoch p , processor i broadcasts the update vector

$$\mathbf{u}_{i,t}^{(p)} = \tilde{Q} \left(\nabla f_{j_{i,t}^{(p)}}(\mathbf{x}_t^{(p)}) - \nabla f_{j_{i,t}^{(p)}}(\mathbf{y}^{(p)}) + H_p \right).$$

Each processor then computes the total update for that iteration $\mathbf{u}_t^{(p)} = \frac{1}{K} \sum_{i=1}^K \mathbf{u}_{t,i}$, and sets $\mathbf{x}_{t+1}^{(p)} = \mathbf{x}_t^{(p)} - \eta \mathbf{u}_t^{(p)}$. At the end of epoch p , each processor sets $\mathbf{y}^{(p+1)} = \frac{1}{T} \sum_{t=1}^T \mathbf{x}_t^{(p)}$.

Our main theorem is that this algorithm still converges, and is communication efficient:

Theorem B.2. *Let $f(\mathbf{x}) = \frac{1}{m} \sum_{i=1}^m f_i(\mathbf{x})$, where f is ℓ -strongly convex, and f_i are convex and L -smooth, for all i . Let \mathbf{x}^* be the unique minimizer of f over \mathbb{R}^n . Then, if $\eta = O(1/L)$ and $T = O(L/\ell)$, then QSVRG with initial point $\mathbf{y}^{(1)}$ ensures*

$$\mathbb{E} \left[f(\mathbf{y}^{(p+1)}) \right] - f(\mathbf{x}^*) \leq 0.9^p \left(f(\mathbf{y}^{(1)}) - f(\mathbf{x}^*) \right). \quad (9)$$

Moreover, QSVRG with P epochs and T iterations per epoch requires $\leq P(F + 2.8n)(T + 1)$ bits of communication per processor.

In particular, observe that when L/ℓ is a constant, this implies that for all epochs p , we may communicate $O(pn)$ bits and get an error rate of the form (14). Up to constant factors, this matches the lower bound given in [40].

Proof of Theorem G.2. By Theorem A.6, each processor transmits at most $F + 2.8n$ bits per iteration, and then an additional $F + 2.8n$ bits per epoch to communicate the $H_{p,i}$. Thus the claimed communication bound follows trivially.

We now turn our attention to correctness. As with the case of quantized SGD, it is not hard to see that the parallel updates are equivalent to minibatched updates, and serve only to decrease the variance of the random gradient estimate. Hence, as before, for simplicity of presentation, we will consider the effect of quantization on convergence rates on a single processor. In this case, the updates can be written down somewhat more simply. Namely, in iteration t of epoch p , we have that

$$\mathbf{x}_{t+1}^{(p)} = \mathbf{x}_t^{(p)} - \eta \tilde{Q}_t^{(p)} \left(\nabla f_{j_t^{(p)}}(\mathbf{x}_t^{(p)}) - \nabla f_{j_t^{(p)}}(\mathbf{y}^{(p)}) + \tilde{Q}^{(p)}(\nabla f(\mathbf{y})) \right),$$

where $j_t^{(p)}$ is a random index of $[m]$, and $\tilde{Q}_t^{(p)}$ and $\tilde{Q}^{(p)}$ are all different, independent instances of \tilde{Q} .

We follow the presentation in [7]. Fix an epoch $p \geq 1$, and let \mathbb{E} denote the expectation taken with respect to the randomness within that epoch.

We will show that

$$\mathbb{E} \left[f(\mathbf{y}^{(p+1)}) \right] - f(\mathbf{x}^*) = \mathbb{E} \left[\frac{1}{T} \sum_{t=1}^T \mathbf{x}_t^{(p)} \right] - f(\mathbf{x}^*) \leq 0.9^p \left(f(\mathbf{y}^{(1)}) - f(\mathbf{x}^*) \right).$$

This clearly suffices to show the theorem. Because we only deal with a fixed epoch, for simplicity of notation, we shall proceed to drop the dependence on p in the notation. For $t = 1, \dots, T$, let $\mathbf{v}_t = \tilde{Q}_t \left(\nabla f_{j_t}(\mathbf{x}_t) - \nabla f_{j_t}(\mathbf{y}) - \tilde{Q}^{(p)}(\nabla f(\mathbf{y})) \right)$ be the update in iteration t . It suffices to show the following two equations:

$$\begin{aligned} \mathbb{E}_{j_t, \tilde{Q}_t, \tilde{Q}} [\mathbf{v}_t] &= \nabla f(\mathbf{x}_t), \text{ and} \\ \mathbb{E}_{j_t, \tilde{Q}_t, \tilde{Q}} [\|\mathbf{v}_t\|^2] &\leq C \cdot L (f(\mathbf{x}_t) - f(\mathbf{x}^*) + f(\mathbf{y}) - f(\mathbf{x}^*)), \end{aligned}$$

where C is some universal constant. That the first equation is true follows from the unbiasedness of \tilde{Q} . We now show the second. We have:

$$\begin{aligned}
\mathbb{E}_{j_t, \tilde{Q}_t, \tilde{Q}} [\|\mathbf{v}_t\|^2] &= \mathbb{E}_{j_t, \tilde{Q}} \mathbb{E}_{\tilde{Q}_s} [\|\mathbf{v}_t\|^2] \\
&\stackrel{(a)}{\leq} 2 \mathbb{E}_{j_t, \tilde{Q}} \left[\left\| \nabla f_{j_t}(\mathbf{x}_t) - \nabla f_{j_t}(\mathbf{y}) + \tilde{Q}^{(p)}(\nabla f(\mathbf{y})) \right\|^2 \right] \\
&\stackrel{(b)}{\leq} 4 \mathbb{E}_{j_t} \left[\|\nabla f_{j_t}(\mathbf{x}_t) - \nabla f_{j_t}(\mathbf{x}^*)\|^2 \right] + 4 \mathbb{E}_{j_t, \tilde{Q}} \left[\left\| \nabla f_{j_t}(\mathbf{x}^*) - \nabla f_{j_t}(\mathbf{y}) + \tilde{Q}^{(p)}(\nabla f(\mathbf{y})) \right\|^2 \right] \\
&\stackrel{(c)}{\leq} 4 \mathbb{E}_{j_t} \left[\|\nabla f_{j_t}(\mathbf{x}_t) - \nabla f_{j_t}(\mathbf{x}^*)\|^2 \right] + 4 \mathbb{E}_{j_t, \tilde{Q}} \left[\|\nabla f_{j_t}(\mathbf{x}^*) - \nabla f_{j_t}(\mathbf{y}) + \nabla f(\mathbf{y})\|^2 \right] \\
&\quad + 4 \mathbb{E}_{j_t, \tilde{Q}} \left[\left\| \nabla f(\mathbf{y}) - \tilde{Q}^{(p)}(\nabla f(\mathbf{y})) \right\|^2 \right] \\
&\stackrel{(d)}{\leq} 4 \mathbb{E}_{j_t} \left[\|\nabla f_{j_t}(\mathbf{x}_t) - \nabla f_{j_t}(\mathbf{x}^*)\|^2 \right] + 4 \mathbb{E}_{j_t, \tilde{Q}} \left[\|\nabla f_{j_t}(\mathbf{x}^*) - \nabla f_{j_t}(\mathbf{y}) + \nabla f(\mathbf{y})\|^2 \right] \\
&\quad + 8 \|\nabla f(\mathbf{y})\|^2 \\
&\stackrel{(e)}{\leq} 8L(f(\mathbf{x}_t) - f(\mathbf{x}^*)) + 4L(f(\mathbf{y}) - f(\mathbf{x}^*)) + 16L(f(\mathbf{y}) - f(\mathbf{x}^*)) \\
&\leq C \cdot L(f(\mathbf{x}_t) - f(\mathbf{x}^*) + f(\mathbf{y}) - f(\mathbf{x}^*)),
\end{aligned}$$

as claimed, for some positive constant $C \leq 16$. Here (a) follows from Lemma 3.1, (b) and (c) follow from the fact that $(a+b)^2 \leq 2a^2 + 2b^2$ for all scalars a, b , (d) follows from Lemma 3.1 and independence, and (e) follows from Lemma 6.4 in [7] and the standard fact that $\|\nabla f(\mathbf{y})\|^2 \leq 2L(f(\mathbf{y}) - f(\mathbf{x}^*))$ if f is ℓ -strongly convex.

Plugging these bounds into proof structure in [7] yields the proof of G.1, as claimed. \square

Why does naive quantization not achieve this rate? Our analysis shows that quantized SVRG achieves the communication efficient rate, using roughly 2.8 times as many bits per iteration, and roughly $C/2 = 8$ times as many iterations. This may beg the question why naive quantization schemes (say, quantizing down to 16 or 32 bits) fails. At a high level, this is because any such quantization can inherently only achieve up to constant error, since the stochastic gradients are always biased by a (small) constant. To circumvent this, one may quantize down to $O(\log 1/\epsilon)$ bits, however, this only matches the upper bound given by [40], and is off from the optimal rate (which we achieve) by a logarithmic factor.

C Quantization for Non-convex SGD

As stated previously, our techniques are portable, and apply easily to a variety of settings where SGD is applied. As a demonstration of this, we show here how we may use quantization on top of recent results which show that SGD converges to local minima when applied on smooth, non-convex functions.

Throughout this paper, our theory only considers the case when f is a convex function. In many interesting applications such as neural network training, however, the objective is non-convex, where much less is known. However, there has been an interesting line of recent work which shows that SGD at least always provably converges to a local minima, when f is smooth. For instance, by applying Theorem 2.1 in [15], we immediately obtain the following convergence result for quantized SGD. Let Q_s be the quantization function defined in Section 3.1. Here we will only state the convergence bound; the communication complexity per iteration is the same as in 3.1.

Theorem C.1. *Let $f : \mathbb{R}^n \rightarrow \mathbb{R}$ be a L -smooth (possibly nonconvex) function, and let \mathbf{x}_1 be an arbitrary initial point. Let $T > 0$ be fixed, and $s > 0$. Then there is a random stopping time R supported on $\{1, \dots, N\}$ so that QSGD with quantization function Q_s , and constant stepsizes $\eta = O(1/L)$ and access to stochastic gradients of f with second moment bound B satisfies*

$$\frac{1}{L} \mathbb{E} [\|\nabla f(\mathbf{x})\|_2^2] \leq O \left(\frac{\sqrt{L(f(\mathbf{x}_1) - f^*)}}{N} + \frac{(1 + \min(n/s^2, \sqrt{n}/s))B}{L} \right).$$

Table 2: Description of networks.

Network	Dataset	Epochs	Parameters	Init. L. Rate	Minibatch size (2, 4, 8, 16 GPUs)
AlexNet	ImageNet	112	62M	0.07	Varies (256, 512, 1024, 1024)
BN-Inception	ImageNet	300	11M	3.6	Varies (256, 256, 256, 1024)
ResNet152	ImageNet	120	60M	1	Varies (32, 64, 128, 256)
VGG19	ImageNet	80	143M	0.1	Varies (64, 128, 256)
ResNet110	CIFAR-10	160	1M	0.1	128
LSTM	AN4	20	13M	0.5	256

Observe that the only difference in the assumptions in [15] from what we generally assume is that they assume a variance bound on the stochastic gradients, whereas we prefer a second moment bound. Hence our result applies immediately to their setting.

Another recent result [29] demonstrates local convergence for SGD for smooth non-convex functions in asynchronous settings. The formulas there are more complicated, so for simplicity we will not reproduce them here. However, it is not hard to see that quantization affects the convergence bounds there in a manner which is parallel to Theorem 3.2.

D Asynchronous QSGD

We consider an asynchronous parameter-server model [28], modelled identically as in [29, Section 3]. In brief, the system consists of a star-shaped network, with a central parameter server, communicating with worker nodes, which exchange information with the master independently and simultaneously. Asynchrony consists of the fact that competing updates might be applied by the master to the shared parameter (but workers always get a consistent version of the parameter).

In this context, the following follows from [29, Theorem 1]:

Theorem D.1. *Let $f : \mathbb{R}^n \rightarrow \mathbb{R}$ be a L -smooth (possibly nonconvex) function, and let x_1 be an arbitrary initial point. Assume unbiased stochastic gradients, with bounded variance σ^2 , and Lipschitzian gradient with parameter L . Let K be the number of iterations, and M be the minibatch size. Further assume that all the locations of the gradient updates $\{\xi_{k,m}\}_{k=[K],m=[M]}$ are independent random variables, and that the delay with which each update is applied is upper bounded by a parameter T . Finally, assume that the steplength sequence $\{\gamma_k\}_{k=[K]}$ satisfies*

$$LM\gamma_k + 2L^2M^2T\gamma_k \sum_{\kappa=1}^T \gamma_{k+\kappa} \leq 1, \forall k = 1, 2, \dots$$

We then have the following ergodic convergence rate for the iteration of QSGD with quantization function Q_s . Let $\gamma = \sum_{k=1}^K \gamma_k$, and $\sigma_s = (1 + \min(n/s^2, \sqrt{n}/s))\sigma$. Then:

$$\sum_{k=1}^K \frac{\gamma_k \mathbb{E}[\|\nabla f(x_k)\|]}{\gamma} \leq \frac{2(f(x_1) - f(x^*)) + \sum_{k=1}^K \left(\gamma_k^2 ML + 2L^2M^2\gamma_k \sum_{j=k-T}^{k-1} \gamma_j^2 \right) \sigma_s^2}{M\gamma}.$$

E Experiments

We now empirically validate our approach on data-parallel GPU training of deep neural networks.

Setup. We performed experiments on Amazon EC2 p2.16xlarge instances, using up to 16 NVIDIA K80 GPUs. Instances have GPUDirect peer-to-peer communication, but do not currently support NVIDIA NCCL extensions. We have implemented QSGD on GPUs using the Microsoft Cognitive Toolkit (CNTK) [3]. This package provides efficient (MPI-based) GPU-to-GPU communication, and implements an optimized version of 1bit-SGD [35]. Our code is released both as open-source and as a docker instance.

We do not quantize small gradient matrices in QSGD, since the computational cost of quantizing small matrices significantly exceeds the reduction in communication from quantization. However,

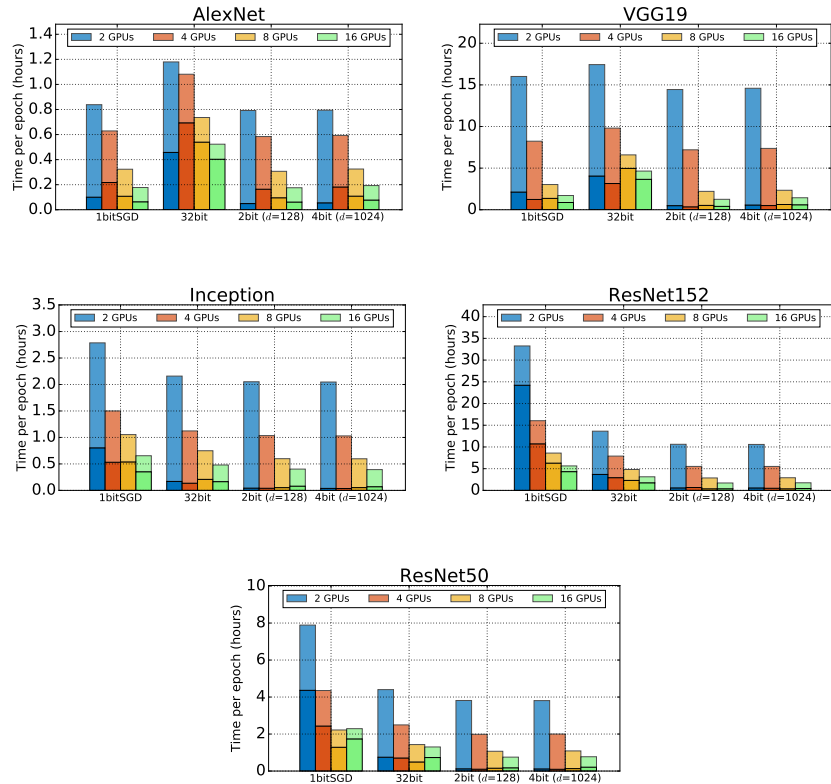


Figure 4: Breakdown of communication versus computation for various neural networks, on 2, 4, 8, 16 GPUs, for full 32-bit precision versus 1BitSGD versus QSGD 2-bit and 4-bit. Each bar represents the total time for an epoch under standard parameters. Epoch time is broken down into *communication* (bottom, solid color) and *computation* (top, transparent color). Notice that, although epoch time usually diminishes as we increase parallelism, the proportion of communication cost increases.

in all experiments, at least 99% of all parameters are transmitted in quantized form. If required, we reshape matrices to fit bucket sizes.

We execute two types of tasks: *image classification* on the ILSVRC (ImageNet) [12], CIFAR-10 [25], and MNIST [27] datasets, and *speech recognition* on the CMU AN4 dataset [2]. For vision, we experimented with AlexNet [26], VGG [36], ResNet [18], and Inception with Batch Normalization [22] deep networks. For speech, we trained an LSTM network [19]. See Table 1.

We used standard sizes for the networks, with hyper-parameters optimized for the 32bit precision variant.¹ Full details for networks and experiments are given in the additional material. We increased batch size when necessary to balance communication and computation for larger GPU counts, and we employed *double buffering* [35] to perform communication and quantization concurrently with the computation. Quantization usually benefits from lowering learning rates; yet, we always run the 32bit learning rate, and decrease bucket size to reduce variance if needed.

Communication vs. Computation. In the first set of experiments, we examine the ratio between computation and communication costs during training, for increased parallelism. The image classification networks are trained on ImageNet, while LSTM is trained on AN4. We examine the cost breakdown for these networks over a pass over the dataset (epoch). Figure 2 gives image classification results. The variance of epoch times is practically negligible.

¹Unless otherwise stated, we use the default networks and hyper-parameters available in the open-source CNTK 2.0.

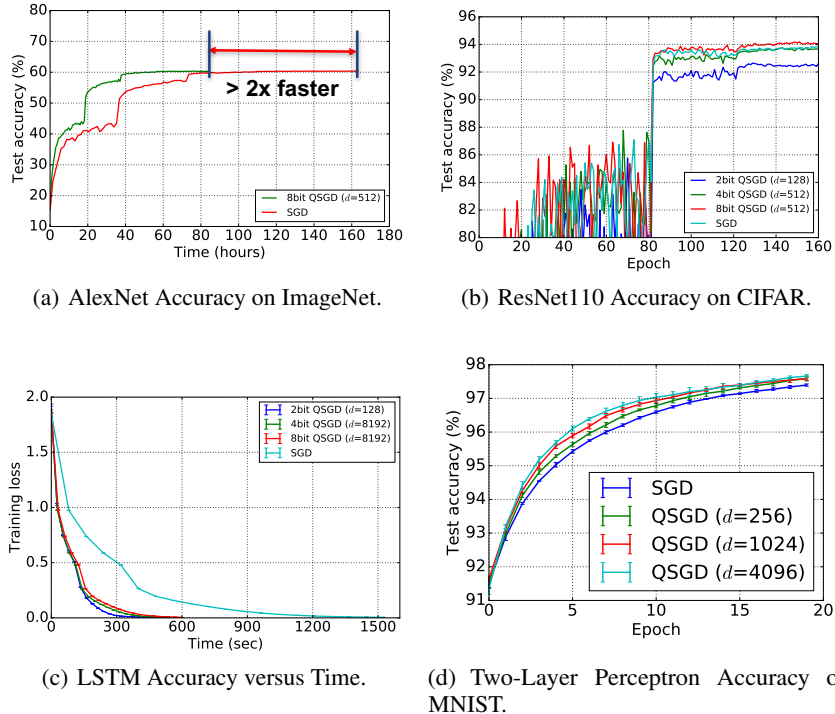


Figure 5: Accuracy numbers for different networks. The red lines in (a) represent final 32-bit accuracy.

The data leads to some interesting observations. First, based on the ratio of communication to computation, we can roughly split networks into *communication-intensive* (AlexNet, VGG, LSTM), and *computation-intensive* (Inception, ResNet). For both network types, the relative impact of communication *increases significantly* as we increase the number of GPUs. Examining the breakdown for the 32-bit version, all networks could significantly benefit from reduced communication. For example, for AlexNet on 16 GPUs with batch size 1024, more than 80% of training time is spent on communication, whereas for LSTM on 2 GPUs with batch size 256, the proportion is 71% communication.²

Next, we examine the impact of QSGD on communication and overall training time. (For QSGD, communication time includes time spent compressing and uncompressing gradients.) We measured QSGD with 2-bit quantization and 64 bucket size, and 4-bit quantization and 8192 bucket size. The results for these two variants are similar, since the different bucket sizes mean that the 4bit version only sends 77% more data than the 2-bit version (but $\sim 8\times$ less than 32-bit). These bucket sizes are chosen to ensure good convergence, but are not carefully tuned.

On 16GPU AlexNet with batch size 1024, 4-bit QSGD reduces communication time by $4\times$, and overall epoch time by $2.5\times$. On LSTM, it reduces communication time by $6.8\times$, and overall epoch time by $2.7\times$. Runtime improvements are non-trivial for all architectures we considered.

Accuracy. We now examine how QSGD influences accuracy and convergence rate. We ran AlexNet to full convergence on ImageNet, LSTM on AN4, ResNet110 on CIFAR-10, as well as a two-layer perceptron on MNIST. Results are given in Figure 5.

On ImageNet using AlexNet, 4-bit QSGD with 8192 bucket size converges to 59.22% top-1 error, and 81.63% top-5 error. The gap from the 32bit version is 0.57% for top-5, and 0.68% for top-1 [9]. QSGD with 2-bit and 64 bucket size has gap 1.73% for top-1, and 1.18% for top-1. We note that we did not tune bucket size, number of bits used, number of epochs or learning rate for this experiment.

²These ratios can be improved by increasing batch size. However, increasing batch size further hurts convergence and decreases accuracy, see also e.g. [21].

```

Data: Parameter vector  $x$ 
1 procedure GradientDescent
2 for each iteration  $t$  do
3    $Q(\nabla f(x)) \leftarrow \text{Quantize}(\nabla f(x))$  //quantize gradient
4    $x \leftarrow x - \eta_t Q(\nabla f(x))$  //apply gradient
5 end

```

Algorithm 2: The gradient descent algorithm with gradient encoding.

On AN4 using LSTMs, 2-bit QSGD has similar convergence rate and the same accuracy as 32bit. It is able to converge $3\times$ faster to the target accuracy with respect to full precision, thanks to reduced communication overheads. The 4-bit variant has the same convergence and accuracy, but is slightly slower than 2-bit (by less than 10%).

On CIFAR-10, 2-bit QSGD applied to ResNet-110 drops about 1.22% top-1 accuracy points. However, 4-bit QSGD converges to the same accuracy as the original, whereas 8-bit QSGD *improves* accuracy by 0.33%. We observe a similar result on MNIST, where 2-bit QSGD with buckets equal to the size of hidden layers improves accuracy by 0.5%. These results are consistent with recent work [30] noting benefits of added noise in training deep networks. Linear models on e.g. MNIST do not show such improvements.

One issue we examined in more detail is which layers are more sensitive to quantization. It appears that quantizing *convolutional layers* too aggressively (e.g., 2-bit precision) can lead to accuracy loss if not trained further. However, increasing precision to 4-bit or 8-bit recovers accuracy. This finding suggests that modern architectures for vision tasks, such as ResNet or Inception, which are almost entirely convolutional, may benefit less from quantization than recurrent deep networks such as LSTMs.

Comparison with 1BitSGD. We have also compared against the 1BitSGD algorithm of [35]. Before discussing results, it is important to note some design choices made in the CNTK implementation of 1BitSGD. For objects without dynamic dimensions, the first tensor dimension is the “row” while the rest are flattened onto “columns.” At the same time, 1BitSGD always quantizes *per column*. In practice, this implies that quantization is often applied to a column of very small dimension (1–3), especially in the case of networks with many convolutions. This has the advantage of having extremely low variance, but does not yield any communication benefits. In fact, it can hurt performance due to the cost of quantization. (By contrast, we reshape to quantize on large dimensions.)

Given this artefact, 1BitSGD is slower than even the 32bit version on heavily convolutional networks such as ResNet and Inception. However, 1BitSGD matches the performance of 2-bit and 4-bit QSGD on AlexNet, VGG, and LSTMs within 10%. In general, 1BitSGD attains very good accuracy (on par with 32bit), probably since the more delicate convolutional layers are not quantized. QSGD has the advantage of being able to perform quantization *on the fly*, without error accumulation: this saves memory, since we do not need to allocate an additional model copy.

F Quantized Gradient Descent: Description and Analysis

In this section, we consider the effect of lossy compression on standard (non-stochastic) gradient descent. Since this procedure is not data-parallel, we will first have to modify the blueprint for the iterative procedure, as described in Algorithm 2. In particular, we assume that, instead of directly applying the gradient to the iterate x_{t+1} , the procedure first *quantizes* the gradient, before applying it. This setting models a scenario where the model and the computation are performed by different machines, and we wish to reduce the communication cost of the gradient updates.

We now give a quantization function tailored for gradient descent, prove convergence of gradient descent with quantization, and then finally bound the length of the encoding.

The Quantization Function. We consider the following *deterministic* quantization function, inspired by [35]. For any vector $\mathbf{v} \in \mathbb{R}^n$, let $I(\mathbf{v})$ be the smallest set of indices of \mathbf{v} such that

$$\sum_{i \in I(\mathbf{v})} |v_i| \geq \|\mathbf{v}\|.$$

Further, define $Q(\mathbf{v})$ to be the vector

$$Q(\mathbf{v})_i = \begin{cases} \|\mathbf{v}\| & \text{if } x \geq 0 \text{ and } i \in I(\mathbf{v}); \\ -\|\mathbf{v}\| & \text{if } x < 0 \text{ and } i \in I(\mathbf{v}); \\ 0 & \text{otherwise.} \end{cases}$$

Practically, we preserve the sign for each index in $I(\mathbf{v})$, the 2-norm of \mathbf{v} , and cancel out all remaining components of \mathbf{v} .

Convergence Bound. We begin by proving some properties of our quantization function. We have the following:

Lemma F.1. *For all $\mathbf{v} \in \mathbb{R}^n$, we have*

1. $\mathbf{v}^T Q(\mathbf{v}) \geq \|\mathbf{v}\|^2$,
2. $|I(\mathbf{v})| \leq \sqrt{n}$, and
3. $\|Q(\mathbf{v})\|^2 \leq \sqrt{n} \|\mathbf{v}\|^2$.

Proof. For the first claim, observe that $\mathbf{v}^T Q(\mathbf{v}) = \|\mathbf{v}\| \sum_{i \in I(\mathbf{v})} |v_i| \geq \|\mathbf{v}\|^2$.

We now prove the second claim. Let $\mathbf{v} = (v_1, \dots, v_n)$, and without loss of generality, assume that $|v_i| \geq |v_{i+1}|$ for all $i = 1, \dots, n-1$, so that the coordinates are in decreasing order. Then $I(\mathbf{v}) = \{1, \dots, D\}$ for some D .

We show that if $D \geq \sqrt{n}$ then $\sum_{i=1}^D |v_i| \geq \|\mathbf{v}\|$, which shows that $|I(\mathbf{v})| \leq \sqrt{n}$. Indeed, we have that

$$\begin{aligned} \left(\sum_{i=1}^D |v_i| \right)^2 &= \sum_{i=1}^D v_i^2 + \sum_{\substack{i \neq j \\ i, j \leq D}} |v_i| |v_j| \\ &\geq \sum_{i=1}^D v_i^2 + (D^2 - D) v_{D+1}^2. \end{aligned}$$

On the other hand, we have

$$\begin{aligned} \|\mathbf{v}\|^2 &= \sum_{i=1}^D v_i^2 + \sum_{D+1}^n v_i^2 \\ &\leq \sum_{i=1}^D v_i^2 + (n - D) v_{D+1}^2 \end{aligned}$$

and so we see that if $D = \sqrt{n}$, we must have $\left(\sum_{i=1}^D |v_i| \right)^2 \geq \|\mathbf{v}\|^2$, as claimed.

For the third claim, observe that $\|Q(\mathbf{v})\|^2 = \|\mathbf{v}\|^2 \cdot |I(\mathbf{v})|$; thus the claim follows from the previous upper bound on the cardinality of $I(\mathbf{v})$. \square

To establish convergence of the quantized method, we prove the following theorem.

Theorem F.2. *Let $f : \mathbb{R}^n \rightarrow \mathbb{R}$ be a ℓ -strongly convex, L -smooth function, with global minimizer \mathbf{x}^* , and condition number $\kappa = L/\ell$. Then, for all step sizes η satisfying $\eta \leq O\left(\frac{\ell}{L^2 \sqrt{n}}\right)$, for all $T \geq 1$, and all initial points \mathbf{x}_0 , we have*

$$f(\mathbf{x}_T) - f(\mathbf{x}^*) \leq \exp\left(-\Omega\left(\frac{1}{\kappa^2 \sqrt{n}}\right) T\right) (f(\mathbf{x}_0) - f(\mathbf{x}^*)).$$

Proof. We first establish the following two properties:

Lemma F.3. *Let f be ℓ -strongly convex and L -smooth. Then,*

1. for all $\mathbf{x} \in \mathbb{R}^n$,

$$\frac{\ell}{2} \|\mathbf{x} - \mathbf{x}^*\|^2 \leq f(\mathbf{x}) - f(\mathbf{x}^*) \leq \frac{L}{2} \|\mathbf{x} - \mathbf{x}^*\|^2 .$$

2. for all $\mathbf{x} \in \mathbb{R}^n$,

$$\nabla f(\mathbf{x})^T Q(\nabla f(\mathbf{x})) \geq \ell(f(\mathbf{x}) - f(\mathbf{x}^*)) .$$

Proof. The first property follows directly from the definitions of strong convexity and smoothness. We now show the second property. If $\mathbf{x} = \mathbf{x}^*$ the property trivially holds so assume that this does not happen. By Lemma F.1, we have

$$\nabla f(\mathbf{x})^T Q(\nabla f(\mathbf{x})) \geq \|\nabla f(\mathbf{x})\|^2 .$$

We then have

$$f(\mathbf{x}) - f(\mathbf{x}^*) \leq \nabla f(\mathbf{x})^T (\mathbf{x} - \mathbf{x}^*) \leq \|\nabla f(\mathbf{x})\| \|\mathbf{x} - \mathbf{x}^*\| ,$$

where the first inequality follows from convexity, and the second from Cauchy-Schwartz. From strong convexity we then have that $\frac{\ell}{2} \|\mathbf{x} - \mathbf{x}^*\|^2 \leq \nabla f^T(\mathbf{x})(\mathbf{x} - \mathbf{x}^*)$ from which we get that

$$\frac{\ell}{2} \|\mathbf{x} - \mathbf{x}^*\| \leq \nabla f(\mathbf{x})^T \frac{\mathbf{x} - \mathbf{x}^*}{\|\mathbf{x} - \mathbf{x}^*\|} \leq \|\nabla f(\mathbf{x})\| ,$$

where the last line follows since from self-duality of the 2-norm, we know that for all vectors $\mathbf{v} \in \mathbb{R}^n$, we have $\|\mathbf{v}\|_2 = \sup_{\|\mathbf{u}\|=1} \mathbf{v}^T \mathbf{u}$. Putting these two things together yields that

$$f(\mathbf{x}) - f(\mathbf{x}^*) \leq \frac{2}{\ell} \|\nabla f(\mathbf{x})\|^2 \leq \frac{2}{\ell} \nabla f(\mathbf{x})^T Q(\nabla f(\mathbf{x})) ,$$

as claimed. \square

With all this in place, we can now complete the proof of the theorem. Fix $t \geq 0$. By applying the lemma, we have:

$$\nabla f(\mathbf{x}_t)^T (\mathbf{x}_{t+1} - \mathbf{x}_t) = -\eta \nabla f(\mathbf{x}_t)^T Q(\nabla f(\mathbf{x}_t)) \leq -\eta \frac{\ell}{2} (f(\mathbf{x}_t) - f(\mathbf{x}^*)) . \quad (10)$$

Moreover, observe that, from standard properties of smooth functions [7], we have

$$\frac{1}{2L} \|\nabla f(\mathbf{x})\|^2 \leq f(\mathbf{x}) - f(\mathbf{x}^*) . \quad (11)$$

Thus, we obtain the following chain of inequalities:

$$\begin{aligned} f(\mathbf{x}_{t+1}) - f(\mathbf{x}_t) &\stackrel{(a)}{\leq} \nabla f(\mathbf{x}_{t+1})^T (\mathbf{x}_{t+1} - \mathbf{x}_t) \\ &= \nabla f(\mathbf{x}_t)^T (\mathbf{x}_{t+1} - \mathbf{x}_t) + (\nabla f(\mathbf{x}_{t+1}) - \nabla f(\mathbf{x}_t))^T (\mathbf{x}_{t+1} - \mathbf{x}_t) \\ &\stackrel{(b)}{\leq} -\eta \frac{\ell}{2} (f(\mathbf{x}_t) - f(\mathbf{x}^*)) + \|\nabla f(\mathbf{x}_{t+1}) - \nabla f(\mathbf{x}_t)\| \|\mathbf{x}_{t+1} - \mathbf{x}_t\| \\ &\stackrel{(c)}{\leq} -\eta \frac{\ell}{2} (f(\mathbf{x}_t) - f(\mathbf{x}^*)) + L \|\mathbf{x}_{t+1} - \mathbf{x}_t\|^2 \\ &= -\eta \frac{\ell}{2} (f(\mathbf{x}_t) - f(\mathbf{x}^*)) + \eta^2 L \|Q(\nabla f(\mathbf{x}_t))\|^2 \\ &\stackrel{(d)}{\leq} -\eta \frac{\ell}{2} (f(\mathbf{x}_t) - f(\mathbf{x}^*)) + \eta^2 L \sqrt{n} \|\nabla f(\mathbf{x}_t)\|_2^2 \\ &\stackrel{(e)}{\leq} -\eta \frac{\ell}{2} (f(\mathbf{x}_t) - f(\mathbf{x}^*)) + \eta^2 2L^2 \sqrt{n} (f(\mathbf{x}_t) - f(\mathbf{x}^*)) \\ &= \left(-\eta \frac{\ell}{2} + 2\eta^2 L^2 \sqrt{n} \right) (f(\mathbf{x}_t) - f(\mathbf{x}^*)) , \end{aligned}$$

where (a) follows from the convexity of f , (b) follows from Equation 10 and the Cauchy-Schwarz inequality, (c) follows from the L -smoothness of f , (d) follows from Lemma F.1, and (e) follows from Equation 11. By our choice of η , we know that the RHS of Equation 12 is negative. Hence, by Lemma F.3 and the definition of η , we have

$$f(\mathbf{x}_{t+1}) - f(\mathbf{x}_t) \leq -\Omega\left(\frac{1}{\kappa^2\sqrt{n}}\right) (f(\mathbf{x}_T) - f(\mathbf{x}^*)) . \quad (12)$$

Letting $\delta_t = f(\mathbf{x}_t) - f(\mathbf{x}^*)$, and observing that $f(\mathbf{x}_{t+1}) - f(\mathbf{x}_t) = \delta_{t+1} - \delta_t$, we see that Equation 12 is equivalent to the statement that

$$\delta_{t+1} \leq \left(1 - \Omega\left(\frac{1}{\kappa^2\sqrt{n}}\right)\right) \delta_t .$$

Thus altogether we have

$$\begin{aligned} \delta_T &\leq \left(1 - \Omega\left(\frac{1}{\kappa^2\sqrt{n}}\right)\right)^T \delta_0 \\ &\leq \exp\left(-\Omega\left(\frac{1}{\kappa^2\sqrt{n}}\right) T\right) \delta_0 , \end{aligned}$$

as claimed. \square

Encoding Length. We obtain the following:

Theorem F.4. *Let $\mathbf{v} \in \mathbb{R}^n$. Then*

$$|\text{Code}(Q(\mathbf{v}))| \leq \sqrt{n}(\log(n) + 1 + \log(e)) + F.$$

G Quantized SVRG

Variance Reduction for Sums of Smooth Functions. One common setting in which SGD sees application in machine learning is when f can be naturally expressed as a sum of smooth functions. Formally, we assume that $f(\mathbf{x}) = \frac{1}{m} \sum_{i=1}^m f_i(\mathbf{x})$. When f can be expressed as a sum of smooth functions, this lends itself naturally to SGD. This is because a natural stochastic gradient for f in this setting is, on input \mathbf{x} , to sample a uniformly random index i , and output $\nabla f_i(\mathbf{x})$. We will also impose somewhat stronger assumptions on f and f_1, f_2, \dots, f_m , namely, that f is strongly convex, and that each f_i is convex and smooth.

Definition G.1 (Strong Convexity). Let $f : \mathbb{R}^n \rightarrow \mathbb{R}$ be a differentiable function. We say that f is ℓ -strongly convex if for all $x, y \in \mathbb{R}^n$, we have

$$f(x) - f(y) \leq \nabla f(x)^T(x - y) - \frac{\ell}{2} \|x - y\|_2^2 .$$

Observe that when $\ell = 0$ this is the standard definition of convexity.

Note that it is well-known that even if we impose these stronger assumptions on f and f_1, f_2, \dots, f_m , then by only applying SGD one still cannot achieve exponential convergence rates, i.e. error rates which improve as $\exp(-T)$ at iteration T . (Such a rate is known in the optimization literature as *linear* convergence.) However, an epoch-based modification of SGD, known as stochastic variance reduced gradient descent (SVRG) [23], is able to give such rates in this specific setting. We describe the method below, following the presentation of Bubeck [7].

Background on SVRG. Let $\mathbf{y}^{(1)} \in \mathbb{R}^n$ be an arbitrary point. For $p = 1, 2, \dots, P$, we let $\mathbf{x}_1^{(p)} = \mathbf{y}^{(p)}$. Each p is called an *epoch*. Then, within epoch p , for $t = 1, \dots, T$, we let $i_t^{(p)}$ be a uniformly random integer from $[m]$ completely independent from everything else, and we set:

$$\mathbf{x}_{t+1}^{(p)} = \mathbf{x}_t^{(p)} - \eta \left(\nabla f_{i_t^{(p)}}(\mathbf{x}_t^{(p)}) - \nabla f_{i_t^{(p)}}(\mathbf{y}^{(p)}) + \nabla f(\mathbf{y}^{(p)}) \right) .$$

We then set

$$\mathbf{y}^{(p+1)} = \frac{1}{k} \sum_{i=1}^k \mathbf{x}_i^{(p)} .$$

With this iterative scheme, we have the following guarantee:

Theorem G.1 ([23]). *Let $f(\mathbf{x}) = \frac{1}{m} \sum_{i=1}^m f_i(\mathbf{x})$, where f is ℓ -strongly convex, and f_i are convex and L -smooth, for all i . Let \mathbf{x}^* be the unique minimizer of f over \mathbb{R}^n . Then, if $\eta = O(1/L)$ and $T = O(L/\ell)$, we have*

$$\mathbb{E} \left[f(\mathbf{y}^{(p+1)}) \right] - f(\mathbf{x}^*) \leq 0.9^p \left(f(\mathbf{y}^{(1)}) - f(\mathbf{x}^*) \right). \quad (13)$$

Quantized SVRG. In parallel SVRG, we are given K processors, each processor i having access to $f_{im/K}, \dots, f_{(i+1)m/K-1}$. The goal is the same as before: to approximately minimize $f = \frac{1}{m} \sum_{i=1}^m f_i$. For processor i , let $h_i = \frac{1}{m} \sum_{j=im/K}^{(i+1)m/K-1} f_j$ be the portion of f that it knows, so that $f = \sum_{i=1}^K h_i$.

A natural question is whether we can apply randomized quantization to reduce communication for parallel SVRG. Whenever one applies our quantization functions to the gradient updates in SVRG, the resulting update is no longer an update of the form used in SVRG, and hence the analysis for SVRG does not immediately give any results in black-box fashion. Instead, we prove that despite this technical issue, one can quantize SVRG updates using our techniques and still obtain the same convergence bounds.

Let $\tilde{Q}(\mathbf{v}) = Q(\mathbf{v}, \sqrt{n})$, where $Q(\mathbf{v}, s)$ is defined as in Section 3.1. Our quantized SVRG updates are as follows. Given arbitrary starting point \mathbf{x}_0 , we let $\mathbf{y}^{(1)} = \mathbf{x}_0$. At the beginning of epoch p , each processor broadcasts

$$H_{p,i} = \tilde{Q} \left(\frac{1}{m} \sum_{j=im/K}^{(i+1)m/K-1} \nabla f_j(\mathbf{y}^{(p)}) \right) = \tilde{Q}(\nabla h_i),$$

from which the processors collectively form $H_p = \sum_{i=1}^m H_{p,i}$ without additional communication. Within each epoch, for each iteration $t = 1, \dots, T$, and for each processor $i = 1, \dots, K$, we let $j_{i,t}^{(p)}$ be a uniformly random integer from $[m]$ completely independent from everything else. Then, in iteration t in epoch p , processor i broadcasts the update vector

$$\mathbf{u}_{t,i}^{(p)} = \tilde{Q} \left(\nabla f_{j_{i,t}^{(p)}}(\mathbf{x}_t^{(p)}) - \nabla f_{j_{i,t}^{(p)}}(\mathbf{y}^{(p)}) + H_p \right).$$

Each processor then computes the total update for that iteration $\mathbf{u}_t^{(p)} = \frac{1}{K} \sum_{i=1}^K \mathbf{u}_{t,i}^{(p)}$, and sets $\mathbf{x}_{t+1}^{(p)} = \mathbf{x}_t^{(p)} - \eta \mathbf{u}_t^{(p)}$. At the end of epoch p , each processor sets $\mathbf{y}^{(p+1)} = \frac{1}{T} \sum_{t=1}^T \mathbf{x}_t^{(p)}$.

Our main theorem is that this algorithm still converges, and is communication efficient:

Theorem G.2. *Let $f(\mathbf{x}) = \frac{1}{m} \sum_{i=1}^m f_i(\mathbf{x})$, where f is ℓ -strongly convex, and f_i are convex and L -smooth, for all i . Let \mathbf{x}^* be the unique minimizer of f over \mathbb{R}^n . Then, if $\eta = O(1/L)$ and $T = O(L/\ell)$, then QSVRG with initial point $\mathbf{y}^{(1)}$ ensures*

$$\mathbb{E} \left[f(\mathbf{y}^{(p+1)}) \right] - f(\mathbf{x}^*) \leq 0.9^p \left(f(\mathbf{y}^{(1)}) - f(\mathbf{x}^*) \right). \quad (14)$$

Moreover, QSVRG with P epochs and T iterations per epoch requires $\leq P(F + 2.8n)(T + 1)$ bits of communication per processor.

In particular, observe that when L/ℓ is a constant, this implies that for all epochs p , we may communicate $O(pn)$ bits and get an error rate of the form (14). Up to constant factors, this matches the lower bound given in [40].

Proof of Theorem G.2. By Theorem A.6, each processor transmits at most $F + 2.8n$ bits per iteration, and then an additional $F + 2.8n$ bits per epoch to communicate the $H_{p,i}$. Thus the claimed communication bound follows trivially.

We now turn our attention to correctness. As with the case of quantized SGD, it is not hard to see that the parallel updates are equivalent to minibatched updates, and serve only to decrease the variance of the random gradient estimate. Hence, as before, for simplicity of presentation, we will consider the

effect of quantization on convergence rates on a single processor. In this case, the updates can be written down somewhat more simply. Namely, in iteration t of epoch p , we have that

$$\mathbf{x}_{t+1}^{(p)} = \mathbf{x}_t^{(p)} - \eta \tilde{Q}_t^{(p)} \left(\nabla f_{j_t^{(p)}}(\mathbf{x}_t^{(p)}) - \nabla f_{j_t^{(p)}}(\mathbf{y}^{(p)}) + \tilde{Q}^{(p)}(\nabla f(\mathbf{y})) \right),$$

where $j_t^{(p)}$ is a random index of $[m]$, and $\tilde{Q}_t^{(p)}$ and $\tilde{Q}^{(p)}$ are all different, independent instances of \tilde{Q} .

We follow the presentation in [7]. Fix an epoch $p \geq 1$, and let \mathbb{E} denote the expectation taken with respect to the randomness within that epoch.

We will show that

$$\mathbb{E} \left[f(\mathbf{y}^{(p+1)}) \right] - f(\mathbf{x}^*) = \mathbb{E} \left[\frac{1}{T} \sum_{t=1}^T \mathbf{x}_t^{(p)} \right] - f(\mathbf{x}^*) \leq 0.9^p \left(f(\mathbf{y}^{(1)}) - f(\mathbf{x}^*) \right).$$

This clearly suffices to show the theorem. Because we only deal with a fixed epoch, for simplicity of notation, we shall proceed to drop the dependence on p in the notation. For $t = 1, \dots, T$, let $\mathbf{v}_t = \tilde{Q}_t \left(\nabla f_{j_t}(\mathbf{x}_t) - \nabla f_{j_t}(\mathbf{y}) - \tilde{Q}^{(p)}(\nabla f(\mathbf{y})) \right)$ be the update in iteration t . It suffices to show the following two equations:

$$\begin{aligned} \mathbb{E}_{j_t, \tilde{Q}_t, \tilde{Q}} [\mathbf{v}_t] &= \nabla f(\mathbf{x}_t), \text{ and} \\ \mathbb{E}_{j_t, \tilde{Q}_t, \tilde{Q}} [\|\mathbf{v}_t\|^2] &\leq C \cdot L \left(f(\mathbf{x}_t) - f(\mathbf{x}^*) + f(\mathbf{y}) - f(\mathbf{x}^*) \right), \end{aligned}$$

where C is some universal constant. That the first equation is true follows from the unbiasedness of \tilde{Q} . We now show the second. We have:

$$\begin{aligned} \mathbb{E}_{j_t, \tilde{Q}_t, \tilde{Q}} [\|\mathbf{v}_t\|^2] &= \mathbb{E}_{j_t, \tilde{Q}} \mathbb{E}_{\tilde{Q}_s} [\|\mathbf{v}_t\|^2] \\ &\stackrel{(a)}{\leq} 2 \mathbb{E}_{j_t, \tilde{Q}} \left[\left\| \nabla f_{j_t}(\mathbf{x}_t) - \nabla f_{j_t}(\mathbf{y}) + \tilde{Q}^{(p)}(\nabla f(\mathbf{y})) \right\|^2 \right] \\ &\stackrel{(b)}{\leq} 4 \mathbb{E}_{j_t} \left[\|\nabla f_{j_t}(\mathbf{x}_t) - \nabla f_{j_t}(\mathbf{x}^*)\|^2 \right] + 4 \mathbb{E}_{j_t, \tilde{Q}} \left[\left\| \nabla f_{j_t}(\mathbf{x}^*) - \nabla f_{j_t}(\mathbf{y}) + \tilde{Q}^{(p)}(\nabla f(\mathbf{y})) \right\|^2 \right] \\ &\stackrel{(c)}{\leq} 4 \mathbb{E}_{j_t} \left[\|\nabla f_{j_t}(\mathbf{x}_t) - \nabla f_{j_t}(\mathbf{x}^*)\|^2 \right] + 4 \mathbb{E}_{j_t, \tilde{Q}} \left[\|\nabla f_{j_t}(\mathbf{x}^*) - \nabla f_{j_t}(\mathbf{y}) + \nabla f(\mathbf{y})\|^2 \right] \\ &\quad + 4 \mathbb{E}_{j_t, \tilde{Q}} \left[\left\| \nabla f(\mathbf{y}) - \tilde{Q}^{(p)}(\nabla f(\mathbf{y})) \right\|^2 \right] \\ &\stackrel{(d)}{\leq} 4 \mathbb{E}_{j_t} \left[\|\nabla f_{j_t}(\mathbf{x}_t) - \nabla f_{j_t}(\mathbf{x}^*)\|^2 \right] + 4 \mathbb{E}_{j_t, \tilde{Q}} \left[\|\nabla f_{j_t}(\mathbf{x}^*) - \nabla f_{j_t}(\mathbf{y}) + \nabla f(\mathbf{y})\|^2 \right] \\ &\quad + 8 \|\nabla f(\mathbf{y})\|^2 \\ &\stackrel{(e)}{\leq} 8L \left(f(\mathbf{x}_t) - f(\mathbf{x}^*) \right) + 4L \left(f(\mathbf{y}) - f(\mathbf{x}^*) \right) + 16L \left(f(\mathbf{y}) - f(\mathbf{x}^*) \right) \\ &\leq C \cdot L \left(f(\mathbf{x}_t) - f(\mathbf{x}^*) + f(\mathbf{y}) - f(\mathbf{x}^*) \right), \end{aligned}$$

as claimed, for some positive constant $C \leq 16$. Here (a) follows from Lemma 3.1, (b) and (c) follow from the fact that $(a+b)^2 \leq 2a^2 + 2b^2$ for all scalars a, b , (d) follows from Lemma 3.1 and independence, and (e) follows from Lemma 6.4 in [7] and the standard fact that $\|\nabla f(\mathbf{y})\|^2 \leq 2L(f(\mathbf{y}) - f(\mathbf{x}^*))$ if f is ℓ -strongly convex.

Plugging these bounds into proof structure in [7] yields the proof of G.1, as claimed. \square

Why does naive quantization not achieve this rate? Our analysis shows that quantized SVRG achieves the communication efficient rate, using roughly 2.8 times as many bits per iteration, and roughly $C/2 = 8$ times as many iterations. This may beg the question why naive quantization schemes (say, quantizing down to 16 or 32 bits) fails. At a high level, this is because any such quantization can inherently only achieve up to constant error, since the stochastic gradients are always biased by a (small) constant. To circumvent this, one may quantize down to $O(\log 1/\epsilon)$ bits, however, this only matches the upper bound given by [40], and is off from the optimal rate (which we achieve) by a logarithmic factor.